BABEŞ-BOLYAI UNIVERSITY

FACULTY OF CHEMISTRY AND CHEMICAL ENGINEERING

Department of Chemical Engineering

11 Arany János, Cluj – Napoca, Romania, 400028

SUMMARY

RENEWABLE HYDROGEN PRODUCTION METHODS BASED ON BIOMASS PROCESSING

PhD THESIS

Eng. Tasnádi-Asztalos Zsolt

Scientific supervisor

Prof. Dr. Eng. Paul Şerban Agachi

Cluj-Napoca 2016

Contents

Part I – Overview and theoretical background 5
Chapter 1. General aspects 6
1.1 Thesis motivation..... 6
1.2 Thesis objectives 6
1.3 Thesis structure and content 8
Reference: 11
Chapter 2. Hydrogen production and hydrogen based power generation from bioethanol reforming: theoretical aspects 12
2.1 Hydrogen production from catalytic steam reforming of bioethanol: thermodynamic and kinetic analysis .. 12
2.2 Hydrogen production using bioethanol as raw-material: process simulation 17
2.3 Hydrogen based power generation using bioethanol as raw-material: conceptual design 24
Reference: 27
Chapter 3. Hydrogen production and hydrogen based power generation from bioglycerol reforming: theoretical aspects 31
3.1 Hydrogen production from catalytic steam reforming of bioglycerol: thermodynamic analysis 31
3.2 Hydrogen production using bioglycerol as raw-material: process simulation 33
3.3 Hydrogen based power generation using bioglycerol as raw-material: conceptual design 40
3.4 Dynamic simulation of hydrogen production from bioglycerol steam reforming in a continuous flow tubular reactor 43
Reference: 46
Part II – Hydrogen production and hydrogen based power generation from bioethanol……...50
Chapter 4. Hydrogen production with steam reforming of bioethanol 51
4.1. Introduction 51
4.2. Thermodynamic analysis of steam reforming of ethanol..... 51
4.3. Kinetic studies of steam reforming of ethanol 61
4.4. Conclusions 65
Reference: 66
Chapter 5. Hydrogen based power generation from ethanol 69
5.1. Introduction 69
5.2. 300 MWth Hydrogen production from ethanol reforming 69
5.3. Pinch analysis for hydrogen production at industrial scale from crude ethanol.....76
5.4. Hydrogen-based power generation using bioethanol as raw-material: conceptual design ..... .83
5.5. Pinch analysis for hydrogen based power generation from different conceptual design from crude ethanol 88
5.6. Conclusions 96
References: 97
Part III – Hydrogen production and hydrogen based power generation from bioglycerol reforming 100
Chapter 6. Hydrogen production with steam reforming of bioglycerol 101
6.1. Introduction 101
6.2. Thermodynamic analysis of catalytic steam reforming of glycerol 101
6.3. Dynamic simulation of hydrogen production from bio-glycerol steam reforming in a continuous flow tubular reactor 119
6.4. Conclusions 139
Reference: 140
Chapter 7. Hydrogen based power generation from glycerol 141
7.1. Introduction 141
7.2. 300 MWth Hydrogen production from glycerol reforming 142
7.3. Pinch analysis for hydrogen production at industrial scale from different conceptual design from …..... 149

7.4. Hydrogen based power generation from different conceptual design from glycerol 156
7.5. Pinch analysis for hydrogen-based power generation from different conceptual design from crude glycerol 162
7.6. Conclusions 170
References 171
Part IV – Conclusions 173
Chapter 8. General conclusions 174
8.1 Conclusions and future work perspective 174
8.2 Personal contributions 175
8.3 List of publications 177
Abbreviations and Nomenclature 178
Acknowleddgments 180
List of figures 181
List of tables 186

Keywords: hydrogen, steam reforming, auto-thermal reforming, bioethanol, bioglycerol, power

Part I – OVERVIEW AND THEORETICAL BACKGROUND

Chapter 1. General aspects

1.1 Thesis motivation

The present PhD thesis focuses on two possible solutions for hydrogen production (alternative to water electrolysis), based on renewable, second generation, raw-materials. The renewable raw-materials can be the main product or the by-product(s) of the biomass processing (e.g. wood, fruits, vegetables, etc.). These raw-materials present second generation bioethanol derived from biomass fermentation respectively of glycerol, resulting from the production of bio-diesel [1, 2].

In recent years, electricity consumption has had an upward trend due to increasing world population through the development of emerging countries. As a consequence of the increase, in the development of emerging countries, theconsumption of fossil fuels (e.g. petroleum, natural gas, coal) increased as well leading to higher emissions of gases with greenhouse effect[2]. In the last period there have been numerous approaches limit such emissions. According to data from literature, CO_2 emissions from the combustion of fossil fuels in the past 25 years has grown by approximately 33%[3]. For reducing CO_2 emissions respectively for reducing fossil fuel dependence, the attention was focused on renewable raw-materials (e.g. Bio-diesel, wind, solar, biomass) which can be used for power generation.

1.2 Thesis objectives

The main objective of the present PhD thesis is to find investigates and compare different renewable sources for hydrogen production respectively hydrogen-based power generation. During the past few years several renewable biomass resources (e.g. algae, wood). This PhD thesis focuses on two raw-materials (bioethanol and bioglycerol) resulting from biomass processing which can be used for hydrogen production respectively for power generation.

A possible solution for reducing dependence on fossil fuels for generating electricity for hydrogen production would be bioethanol. Bioethanol is the result of fermentation process of biomass (wood chips, fruits and vegetables). After the primary fermentation of biomass results in a ethanol solution of some 20-25% wt. This solution is subjected to a catalytic reforming process. The first step

for industrial-scale production of hydrogen, respectively electricity generation, from catalytic reforming the bioethanol is to conduct a study to determine the conditions of thermodynamics work favorable to high hydrogen purity production. In the next step towards the industrialization process of hydrogen production via catalytic reforming of bioethanol the kinetics of catalytic reforming of ethanol is establish. These steps identify the main reactions starting from the raw-material (bioethanol) to get the main product (hydrogen). The importance of kinetic analysis is the determination of the kinetic constants which influence the reaction speed to maximize the main product and to minimizing the by-products concentrations. After the thermodynamic study respectively the kinetic analysis, the next step is to develop the conceptual design for ethanol reforming. The aim of the fourth step is to produce a sufficient quantity of hydrogen which can be used in a M701G2 gas turbine to generate 334 MW of power. The final step towards streamlining the production of hydrogen respectively energy generation is PINCH analysis.

Another possible solution for the production of renewable hydrogen or renewable electricity generation the usage of the principal byproduct resulting from the production of bio-diesel, moe exactely the usage of glycerin. As a result of increasing production of bio-diesel in the world, a significant amount of glycerol is generated. One of the objectives of the present thesis is to investigate different technological schemes for electricity generation using hydrogen, resulted from catalytic steam reforming of bioglycerol, as raw-material. The first step for industrial-scale production of hydrogen respectively electricity generation from catalytic reforming the bioglycerol is to conduct a study to determine the conditions of thermodynamics work favorable to high hydrogen purity production. In the next step towards the industrialization process of hydrogen production via catalytic reforming of bioglycerol the process kinetic is establish. These steps identify the main reactions that starting from the raw-material (bioglycerol) to get to the main product (hydrogen). The importance of kinetic analysis is the determination of the reaction constants to maximize the main product and to minimizing the by-products concentrations. After the thermodynamic study respectively the kinetic analysis, the next step is to develop the conceptual design for bioglycerol reforming. The aim of the fourth step is to produce a sufficient quantity of hydrogen which can be used in a M701G2 gas turbine to generate 334 MW of power. The final step towards streamlining the production of hydrogen respectively energy generation is PINCH analysis.

1.3 Thesis structure and content

This PhD thesis is divided in four parts as follows:

- Overview and theoretical background
- Hydrogen production and power generation from bioethanol
- Hydrogen production and power generation from bioglycerol
- Conclusions

The first part (Overview and theoretical background) includes the first three chapters of the PhD thesis entitled RENEWABLE HYDROGEN PRODUCTION METHODS BASED ON BIOMASS PROCESSING. These three chapters are as follows:

- Chapter 1. General aspects

- Chapter 2. Hydrogen production and hydrogen-based power generation from bioethanol reforming: theoretical aspects
- Chapter 3. Hydrogen production and hydrogen-based power generation from bioglycerol reforming: theoretical aspects

Chapter 2 consists of three subsections:

- 2.1. Hydrogen production from catalytic steam reforming of bioethanol: thermodynamic and kinetic analysis
- 2.2. Hydrogen production using bioethanol as raw-material: process simulation
- 2.3. Hydrogen based power generation using bioethanol as raw-material: conceptual design

Chapter 3 comprises the following subsections:

- 3.1. Hydrogen production from catalytic steam reforming of bioglycerol: thermodynamic analysis
- 3.2. Hydrogen production using bioglycerol as raw-material: process simulation
- 3.3. Hydrogen based power generation using bioglycerol as raw-material: conceptual design
- 3.4. Dynamic simulation of hydrogen production from bioglycerol steam reforming in a continuous flow tubular reactor

The second part of the thesis is focused on the results of the simulation for hydrogen production from steam reforming catalytic bioethanol. This part consists of two chapters:

- Chapter 4. Hydrogen production from steam reforming of bioethanol
- Chapter 5. Hydrogen-based power generation from ethanol.

The results of the simulations, based on a thermodynamic study, to observe the effects of various parameters (e.g. temperature, pressure, initial molar ratio of the raw-materials) on the component concentration are reported in Chapter 4. This chapter also discusses the kinetic study of the catalytic steam reforming of crude ethanol. The structure of Chapter 4 is the following:

- 4.1. Introduction
- 4.2. Thermodynamic analysis of steam reforming of ethanol
- 4.3. Kinetic studies of steam reforming of ethanol
- 4.4. Conclusions

In Chapter 5 of the thesis various design concepts of catalytic reforming of ethanol for hydrogen production and electricity generation are presented. This chapter also includes the PINCH analysis for the production of 100000 Nm^3 of hydrogen respectively the power generated based on hydrogen. This chapter consists of the following subsections:

- 5.1. Introduction
- 5.2. 300 MW_{th} Hydrogen production from ethanol reforming
- 5.3. Pinch analysis for hydrogen production at industrial scale from bioethanol
- 5.4. Hydrogen based power generation from ethanol: conceptual design
- 5.5. Pinch analysis for hydrogen based power generation from different conceptual design from bioethanol

- 5.6. Conclusions

The third part of the thesis is focused on the results of the simulation for hydrogen production from catalytic steam reforming of bioglycerol. This part consists of two chapters.:

- Chapter 6. Hydrogen production from steam reforming of bioglycerol
- Chapter 7. Hydrogen based power generation from glycerol.

The results of the simulations, based on a thermodynamic study, to observe the effects of various parameters (e.g. temperature, pressure, initial molar ratio of the raw-materials) on the component concentration are reported in Chapter 6. This chapter also discusses the dynamic simulation of hydrogen production from bioglycerol steam reforming in a continuous flow tubular reactor. The structure of Chapter 6 is the following:

- 6.1. Introduction
- 6.2. Thermodynamic analysis of steam reforming of glicerol
- 6.3. Dynamic simulation of hydrogen production from bioglycerol steam reforming in a continuous flow tubular reactor
- 6.4. Conclusions

In Chapter 7 of the thesis various design concepts of catalytic reforming of glycerol for hydrogen production and electricity generation are presented. This chapter also includes PINCH analyses of production 100000Nm^3 of hydrogen respectively power generation based on hydrogen. This chapter consists of the following subsections:

- 7.1. Introduction
- 7.2. 300 MW_{th} Hydrogen production from glycerol reforming
- 7.3. Pinch analysis for hydrogen production at industrial scale from bioglycerol
- 7.4. Hydrogen based power generation from bioglycerol: conceptual design
- 7.5. Pinch analysis for hydrogen based power generation from different conceptual design from bioglycerol
- 7.6. Conclusions

The fourth part contains the Conclusions and is titled chapter of General conclusions which in turn contains three subsections. Chapter 8 includes the following subsections:

- 8.1. Conclusions and future work perspective
- 8.2. Personal contributions
- 8.3. List of publications

Reference (summary):

1. http://ethanolrfa.org/ accessed 09.05.2016
2. Dr. Christoph Berg, F.O. Licht, World Fuel Ethanol Analysis and Outlook

3. https://yearbook.enerdata.net/CO2-emissions-data-from-fuel-combustion.html accessed 09.05.2016

Chapter 2. Hydrogen production and hydrogen based power generation from bioethanol reforming: theoretical aspects

2.1 Hydrogen production from catalytic steam reforming of bioethanol: thermodynamic and kinetic analysis

In this subchapter, a thermodynamic analysis for bioethanol steam reforming for hydrogen production is presented. Bioethanol is a newly proposed renewable energy carrier mainly produced from biomass fermentation. Reforming of bioethanol provides a promising method for hydrogen production from renewable resources. The demand for hydrogen is increasing in recent times because of its wide applications in areas such as the production of chemicals, crude oil refining, heavy oil, oil sands, metallurgy and aerospace propulsion upgrading and as fuel for the proton exchange membrane (PEM) fuel cell [1].

Biomass is proposed as an alternative for the production of hydrogen, because it is an abundant and renewable resource that does not contribute to net increase of CO_2 in the atmosphere.

Steam reforming of ethanol (SRE) takes place under the action of a metal catalyst capable of breaking C-C bonds into smaller molecules [2]. The reaction is highly endothermic with a standard enthalpy, ΔH^0_{298}=+173.3 kJ/mol of ethanol and occurs at relatively higher temperatures typically between 100 and 1000 ^oC. This reaction is considered as a combination of SRE to syngas [1-13]:

$CH_3CH_2OH(g) + 3\ H_2O(g) \rightarrow 6\ H_2(g) + 2\ CO_2(g)$ (1)

$CH_3CH_2OH(g) + H_2O(g) \rightarrow 4\ H_2(g) + 2\ CO\ (g)$ (2)

followed by WGS (*Water Gas Shift* – WGS):

$CO(g) + H_2O(g) \rightarrow CO_2(g) + H_2(g)$ (3)

The following reactions were used in the kinetic study:

E_1: $CH_3CH_2OH(g) \rightarrow H_2(g) + CO(g) + CH_4(g)$. (4)

E_2: $CH_3CH_2OH_{(g)} + H_2O_{(g)} \rightarrow CO_{2(g)} + CH_{4(g)} + 2H_{2(g)}$ (5)

R_1: $CH_4(g) + 2\ H_2O(g) \rightarrow CO_2(g) + 4\ H_2(g)$ (6)

R_2: $CO_{(g)} + H_2O_{(g)} \leftrightarrow CO_{2(g)} + H_{2(g)}$ (7)

There are few papers in the literature on kinetic studies of ethanol steam reforming, because the system complexity. Ethanol was used as the representative component for bioethanol because of its much higher concentration compared to other components that are present in the bioethanol mixture.

Some published kinetic studies used power law, Eley Rideal (ER), Langmuir Hinshelwood (LH) and Langmuir-Hinshelwood-Hougen-Watson (LHHW) as kinetic expressions [2, 12, 14-16]. Empirical and mechanistic rate models were developed to fit the experimental data as follows. Firstly, an empirical, irreversible fixed feed molar ratio power law rate model was developed as shown by the following equation [1, 12]:

$$r_A = k_0 \cdot e^{\left(-\frac{Ea}{R \cdot T}\right)} \cdot N_A^n \quad (8)$$

Secondly, different mechanistic models were developed based on LHHW and ER mechanisms. Fundamentally, LHHW differs from the ER mechanism in that the former requires the adsorption of the

two reactant species on the catalyst active site for any transformation to take place whereas the latter requires only one of the two reactants species to be adsorbed [2, 12, 13].

The criterion used in the selection of the kinetic model was the temperature range and the available kinetic data. Considering these aspects the LHHW kinetic model was selected and used in this thesis.

As it was established, the kinetic model consists only of 4 reactions: E_1, E_2, R_1 and R_2 - reactions (4-7) [12, 14, 17, 18]. The reaction rates for these four reactions are (9-12):

$$r_{E1} = \frac{k_{E1} \cdot y_E \cdot y_{CH4}^{-1} \cdot y_{H2}^{-\left(\frac{1}{2}\right)}}{DEN^2} \tag{9}$$

$$r_{E2} = \frac{k_{E2} \cdot y_E \cdot y_{CH4}^{-1} \cdot y_{H2}^{-1} \cdot y_{H2O}}{DEN^2} \tag{10}$$

$$r_{R1} = \frac{k_{R1} \cdot y_{CH4} \cdot y_{H2O}^{2} \cdot y_{H2}^{-\left(\frac{5}{2}\right)} \cdot (1-\beta_{R1})}{DEN^3} \tag{11}$$

$$r_{R2} = \frac{k_{R2} \cdot y_{CO2} \cdot y_{H2}^{\left(\frac{1}{2}\right)} \cdot (1-\beta_{R2})}{DEN^2} \tag{12}$$

where the *DEN* term of these expressions is defined as:

$$DEN = 1 + K_{Et} \times y_{Et} + K_{Etx} \times y_{Et} \times y_{H2}^{-(1/2)} + K_{Ac} \times y_{Et} \times y_{H2}^{-1} + K_{CHO} \times y_{Et} \times y_{CH4}^{-1} \times y_{H2}^{-(1/2)} + K_{CH3} \times y_{CH4} \times y_{H2}^{-(1/2)} + K_{CH2} \times y_{CH4} \times y_{H2}^{-1} + K_{CH} \times y_{CH4} \times y_{H2}^{-(3/2)} + K_{H2O} \times y_{H2O} + K_{OH} \times y_{H2O} \times y_{H2}^{-(1/2)} + K_{CH4} \times y_{CH4} + K_{CO} \times y_{CO} + K_{CO2} \times y_{CO2} + K_{H2} \times y_{H2}^{1/2} + K_{H2} \times y_{H2} \tag{13}$$

2.2 Hydrogen production using bioethanol as raw-material: process simulation

This thesis evaluates various innovative hydrogen production options using ethanol residues, as feedstock, simultaneous with carbon capture. There are several ethanol reforming possibilities for hydrogen production (e.g. conventional steam reforming, autothermal reforming), as well as carbon capture options (e.g. gas-solid and gas-liquid systems) to be integrated in the overall plant design [19-22]. Steam reforming of ethanol for hydrogen production implies the following global reaction [4-13]:

$$C_2H_5OH + 3H_2O \rightarrow 2CO_2 + 6H_2 \qquad \Delta H = +157 \text{ kJ/mole} \tag{14}$$

The syngas produced from ethanol reforming is then shift converted with steam. The water gas shift (WGS) reaction has a double purpose in overall ethanol reforming process: one to concentrate the syngas energy in form of hydrogen-rich gas and two to transform the carbon species into carbon dioxide which can be then captured by gas-liquid absorption process [19, 23-25]. After carbon capture (pre-combustion capture configuration), the hydrogen-rich gas is purified by Pressure Swing Adsorption (PSA) to the desired specification. This thesis considers hydrogen purity higher than 99.95% (vol.) to be compatible with chemical applications as well as PEM fuel cells. The PSA tail gas and additional hydrogen-rich gas are used, in an external burner, to cover the heat duty of the reforming reaction [19].

Autothermal reforming can also be used for ethanol conversion to hydrogen. Apart of conventional steam reforming, an oxygen stream is used to totally oxidize (exothermic reaction) part of the ethanol to cover the reforming endothermic reaction. In this plant configuration, no external burner is needed for the reforming reactor, the tail gas is used to generate power to cover the ancillary plant consumption. In both steam reforming and autothermal reforming configuration, the available hot

streams are used to generate steam which then is expanded in a steam turbine to produce power. Co-generation of hydrogen and power (both total decarbonized energy vectors) is one additional attractive feature of these conversion routes which is evaluated in this work[19,26].

Another emerging promising carbon capture option to be integrated in energy conversion systems is based on chemical looping. The chemical looping technique consists in two processes (oxidation and reduction) performed in separate but interconnected circulated fluidized bed (CFB) reactors [19, 26-29].

In the reduction step, the fuel is reacting with an oxygen carrier to form carbon dioxide and water. The mixed gas-solid system at the exit of the fuel reactor is separated by a cyclone, the gas phase is processed further and the solid phase is passed to the next reactor in the cycle. The reduced form of the oxygen carrier is furthermore re-oxidized, using steam and/or air and then is recycled back to the fuel reactor. When hydrogen is to be produced, a three reactor system is used [19, 30].

The oxygen carrier re-oxidation is done in steps, first with steam to produce hydrogen and then with air. Both steam and air exothermic reactions are thermally integrated with the fuel conversion (endothermic reaction) [19, 31]. Considering ethanol conversion by an iron-based chemical looping system, the chemical reactions which take place in the cycle are presented below.

- Fuel reactor:

$$Fe_2O_3 + 3CO \rightarrow 2Fe + 3CO_2 \quad (15)$$

$$Fe_2O_3 + 3H_2 \rightarrow 2Fe + 3H_2O \quad (16)$$

$$4Fe_2O_3 + 3CH_4 \rightarrow 8Fe + 3CO_2 + 6H_2O \quad (17)$$

- Steam reactor:

$$3Fe + 4H_2O \rightarrow Fe_3O_4 + 4H_2 \quad (18)$$

- Air reactor:

$$2Fe_3O_4 + 1/2O_2 \rightarrow 3Fe_2O_3 \quad (19)$$

2.3 Hydrogen based power generation using bioethanol as raw-material: conceptual design

This subchapter focuses on electricity generation based on hydrogen which was obtained by catalytic reforming of bioethanol. Hydrogen shall be obtained by catalytic reforming of bioethanol[2], followed by the water-gas shift[3] (WGS) to decrease the amount of CO and to concentrate the H_2 and CO_2[26]. As CO_2 capture method gas-liquid absorption based on methyl-di-ethyl-amine is used. To obtain a high hydrogen purity (99.9% vol.), the gas streams (in both with and without carbon capture concepts) are passed through the pressure swing adsorption (PSA)[26, 32, 33]. The power generation based on hydrogen was achieved with M701G2 gas turbine (Mitsubishi Hitachi Power Systems) [34-36].

Reference (summary):

1. E. Akpan, A. Akande, A. Aboudheir, H. Ibrahim, R. Idem, *Chemical Engineering Science*, **2007,** 62, 3112.
2. K. Liu, C. Song, V. Subramani, “Hydrogen and Syngas Production and Purification Technologies” A John Wiley & Sons, Inc., Publication **2010.**
3. S. Tosti, A. Basile, R. Borelli, F. Borgognoni, S. Castelli, M. Fabbricino, F. Gallucci, C. Licusati, *International Journal of Hydrogen Energy*, **2009**, 34, 4747.

4. M. Ni, D.Y.C. Leung, M.K.H. Leung, *International Journal of Hydrogen Energy*, **2007**, 32, 3238.
5. M. Benito, J.L. Sanz, R. Isabel, R. Padilla, R. Arjona, L. Dazaa, *Journal of Power Sources*, **2005**, 151, 11.
6. L. Hernández, V. Kafarov, *Journal of Power Sources*, **2009**, 192, 195.
7. A. Iulianelli, A. Basile, *International Journal of Hydrogen Energy*, **2010**, 35, 3170.
8. M. Ni, D.Y.C. Leung, M.K.H. Leung, *International Journal of Hydrogen Energy*, **2007**, 32, 3238.
9. V. Mas, G. Baronetti, N. Amadeo, M. Laborde, *Chemical Engineering Journal*, **2008**, 138, 602.
10. P.D. Vaidya and A.E. Rodrigues, *Industrial & Engineering Chemistry Research*, **2006**, *45*, 6614.
11. D.R. Sahoo, S. Vajpai, S. Patel, K.K. Pant , *Chemical Engineering Journal*, **2007**, 125, 139.
12. Zs. Tasnadi-Asztalos**,** A. Imre-Lucaci, A.M. Cormos, M. D. Lazar, P.S. Agaci; *Studia Universitatis Babes - Bolyai, Chemia*, **2013**, LVIII, 4, 101-112,.
13. Zs. Tasnadi-Asztalos**,** A.M. Cormos, Á. Imre-Lucaci, C.C. Cormos, *AIP Conference Proceedings*, **2013**, 175, 1565.
14. I. Llera, V. Mas, M.L. Bergamini, M. Laborde, N. Amadeo, *Chemical Engineering Science*, **2012**, 71, 356.
15. A. Akande, A. Aboudheir, R. Idem, A. Dalai, *Int J Hydrog Energy*, **2006**, 31, 1707.
16. V. Mas, M.L. Bergamini, G. Baronetti, N. Amadeo, M. Laborde, *Top Catal*, **2008**, 51, 39.
17. A.G. Gayubo, A. Alonso, B. Valle, A.T. Aguayo, M. Olazar, J. Bilbao, *Chemical Engineering Journal*, **2011,** 167, 262.
18. O. Görke , P. Pfeifer, K. Schubert, *Applied Catalysis A: General*, **2009**, 360, 232.
19. Zs. Tasnadi-Asztalos, P.-S. Agachi, C.-Cristian Cormos, *Int J Hydrog Energy*, **2015**, 40, 22, 7017.
20. J.M. Silva, M.A. Soria, L.M. Madeira, *Renew Sust Energy Rev*, **2015**, 42, 1187.
21. C.C. Cormos, *Int J Hydrog Energy*, **2014**, 39, 5597.
22. A. Blasi, G. Fiorenza, C. Freda, V. Calabr_o., Steam reforming of biofuels for the production of hydrogen-rich gas. In: Gugliuzza A, Basile A, editors. Membranes for clean and renewable power applications. Woodhead Publishing Limited; **2014**, 145-81.
23. A. Kohl, R. Nielsen, Gas purification. 5th ed. Huston: Gulf Publishing Company; **1997**.
24. P. Padurean, C.C. Cormos, P.S. Agachi, *Int J Greenh Gas Con*, **2011,** 7, 1.
25. C.C. Cormos, A.M. Cormos, S. Agachi, *Asia Pac J Chem Eng*, **2009**, 4, 870.
26. Zs. Tasnadi-Asztalos, C.-C. Cormos, and P.-S. Agachi; *AIP Conference Proceedings*, **2015**, 1700, 050001.
27. L.S. Fan, Chemical looping systems for fossil energy conversions. Hoboken, New Jersey, USA: Wiley-AIChE; JohnWiley & Sons Inc.; **2010**.
28. J. Adanez, A. Abad, F. Garcia-Labiano, P. Gayan, L. de Diego, *Prog Energy Combust*, **2012**, 38, 215.
29. B. Dou, Y. Song, C. Wang, H. Chen, M. Yang, Y. Xu, *Appl Energy*, **2014,** 130, 342.

30. P. Chiesa, G. Lozza, A. Malandrino, M. Romano, V. Picollo, *Int J Hydrog Energy*, **2008,** 33, 2233.
31. C.C. Cormos, *Int J Hydrog Energy*, **2010,** 35, 2278.
32. A. M. Ribeiro, C. A. Grande, F. V. S. Lopes, J. M. Loureiro, A. E. Rodrigues, *Chem Eng Sci*, **2008,** 63, 5258.
33. V. G. Gomes, K. W. K. Yee, *Sep Purif Technol* , **2002,** 28**,** 161
34. Mitsubishi Heavy Industries. MHI Gas Turbine Technology**.** www.mhi-global.com (accessed 15.06.2015)
35. T. Methling, N. Armbrust, T. Haitz, M. Speidel, N. Poboss, M. Braun-Unkhoff, H. Dieter, B. Kempter-Regel, G. Kraaij, U. Schliessmann, Y. Sterr, A. Wörner, T. Hirth, U. Riedel, G. Scheffknecht, *Bioresource Technol*, **2014,** 169**,** 510.
36. A. Thakur, C. E. Canter, A. Kumar, *App Energ*, **2014,** 128**,** 246

Chapter 3. Hydrogen production and hydrogen based power generation from bioglycerol reforming: theoretical aspects

3.1 Hydrogen production from catalytic steam reforming of bioglycerol: thermodynamic analysis

A thermodynamic analysis and experimental literature date validation of bioglycerol catalytic steam reforming process using Ni/Al_2O_3 catalyst for hydrogen production is presented in this subchapter.

Due to continuous increasing energy demand and low stocks of fossil fuels, new sources of energy and fuel are required to be developed. A solution for renewable fuels is based on biodiesel [1, 2]. The main by-product of the process of biodiesel production is glycerol. With increasing production of biodiesel, a glut of glycerol ($C_3H_8O_3$) is expected in the world market and therefore it is essential to find useful applications for glycerol. Currently, glycerol is used in many applications including personal care, food, oral care, tobacco, polymer and pharmaceutical application [3]. Bioglycerol is a newly proposed renewable energy carrier mainly produced from biomass. Reforming of bioglycerol provides a promising method for hydrogen production from renewable resources. Steam reforming of bioglycerol takes place under the action of a metal catalyst capable of breaking C-C bonds into smaller molecules. The overall reaction for steam reforming of glycerol (SRG) is the following [2]:

$$C_3H_8O_3 + 3H_2O \rightarrow 3CO_2 + 7H_2, \qquad \Delta H_{298}=128 \text{ kJ/mol} \qquad (1)$$

The thermodynamic study was performed by developing a mathematical model of the process using the CHEMCAD process simulator a well-known and widely used CAPE tool. All major reactions (1, 3-7, 10-13) and major products (H_2, CO, CO_2, CH_4, C) obtained in the steam reforming of glycerol were considered in the thermodynamic analysis[2].

A thermodynamic study of a process is very important, because process optimization, through sensitivity analysis study, leads to the optimal reaction conditions [3, 4]. The most frequent methods for the thermodynamic analysis is based on the variation of Gibbs free energy (2)[2].

$$dG = \sum_{i=1}^{N} \mu_i dn_i \qquad (2)$$

The thermodynamic analysis was performed in CHEMCAD processes simulator. The major secondary reactions which take place in parallel with steam reforming of glycerol are the following [2, 4-7]:

Reactions where the major by-products are formed:

$C_3H_8O_3 \leftrightarrow 4H_2 + 3CO$ (3)

$CO_2 + CH_4 \leftrightarrow 2H_2 + 2CO$ (4)

$CO + H_2O \leftrightarrow H_2 + CO_2$ (5)

$CO + 3H2 \leftrightarrow CH4 + H2O$ (6)

$CO_2 + 4H_2 \leftrightarrow CH_4 + 2H_2O$ (7)

$C_3H_8O_3 \rightarrow C_3H_6O_2 + H_2O$ (8)

$C_3H_8O_3 \rightarrow C_3H_6O_3 + H_2$ (9)

The main reactions where carbon is formed:

$2CO \rightarrow CO_2 + C$ (10)

$CH_4 \rightarrow 2H_2 + C$ (11)

$CO + H_2 \rightarrow H_2O + C$ (12)

$CO_2 + 2H_2 \rightarrow 2H_2O + C$ (13)

$C_2H_4 \rightarrow 2H_2 + 2C$ (14)

In CHEMCAD (CAPE simulator) the PSRK (Predictive Soave-Redlich-Kwong) thermodynamic model was set[2].

3.2 Hydrogen production using bioglycerol as raw-material: process simulation

Glycerol is the main byproduct from biodiesel production (one ton of glycerol is produced to ten tons of biodiesel) [8,10]. No particular large scale usage for glycerol residues resulted from biodiesel production is available today. The chemical utilization of glycerol residues from biodiesel production is complicated by its low purity (mixture with unreacted methanol, triglycerides, salts and catalysts) and high energy intensity required for distillation [8].

Another energy carrier with good future prospective in energy, chemical and transport sectors is hydrogen. Currently hydrogen is mainly produced from fossil fuels (e.g. coal gasification and natural gas catalytic reforming) [8, 11-13]. Hydrogen is seen as an important energy carrier for the future low carbon economy in combination with renewable sources and decarbonized fossil fuels. Apart of boosting renewable energy sources, Carbon Capture and Storage (CCS) technologies and improving overall energy efficiency of the conversion routes are seen as important methods to develop the future low carbon economy. 30% cut of CO_2 emissions compared to 1990 levels as well as 20% save of predicted energy consumption levels by improving the energy efficiency are targeted to be realized at EU level by 2020 [8,9].

This part of the thesis evaluates various innovative hydrogen production options using glycerol residues, as feedstock, simultaneous with carbon capture. There are several glycerol reforming possibilities for hydrogen production (e.g. conventional steam reforming, autothermal reforming), as well as carbon capture options (e.g. gas-solid and gas-liquid systems) to be integrated in the overall plant design [8, 14, 15]. Glycerol steam reforming for hydrogen production implies the following global reaction [8, 16]:

$$C_3H_8O_3 + 3H_2O \rightarrow 3CO_2 + 7H_2 \quad (15)$$

The syngas produced from glycerol reforming is then shift converted with steam. The water gas shift (WGS) reaction has a double purpose in overall glycerol reforming process: one to concentrate the syngas energy in form of hydrogen-rich gas and the other to transform the carbon species into carbon dioxide which can be then captured by gas-liquid absorption process [8,17-19]. After carbon capture (pre-combustion capture configuration), the hydrogen-rich gas is purified by Pressure Swing Adsorption (PSA) to the desired specification. This work considers hydrogen purity higher than 99.95% (vol.) to be compatible with chemical applications as well as PEM fuel cells. The PSA tail gas and additional hydrogen-rich gas are used, in an external burner, to cover the heat duty of the reforming reaction [8].

Autothermal reforming can also be used for glycerol conversion to hydrogen. Apart of conventional steam reforming, an oxygen stream is used to totally oxidize (exothermic reaction) part of the glycerol to cover the reforming endothermic reaction. In this plant configuration, no external burner is needed for the reforming reactor, the tail gas is used to generate power to cover the ancillary plant consumption. In both steam reforming and autothermal reforming configuration, the available hot streams are used to generate steam which then is expanded in a steam turbine to produce power. Co-generation of hydrogen and power (both total decarbonized energy vectors) is one additional attractive feature of these conversion routes which is evaluated in subchapter[8].

Another emerging promising carbon capture option to be integrated in energy conversion systems is based on chemical looping. The chemical looping technique consists in two processes (oxidation and reduction) performed in separate but interconnected circulated fluidized bed (CFB) reactors [8,20-22].

In the reduction step, the fuel is reacting with an oxygen carrier to form carbon dioxide and water. The mixed gas-solid system at the exit of the fuel reactor is separated by a cyclone, the gas phase is processed further and the solid phase is passed to the next reactor in the cycle. The reduced form of the oxygen carrier is furthermore re-oxidized, using steam and/or air and then is recycled back to the fuel reactor. When hydrogen is to be produced, a three reactor system is used [8, 23].

The oxygen carrier re-oxidation is done in steps, first with steam to produce hydrogen and then with air. Both steam and air exothermic reactions are thermally integrated with the fuel conversion (endothermic reaction) [24]. Considering glycerol conversion by an iron-based chemical looping system, the chemical reactions which take place in the cycle are presented below [8].

- Fuel reactor:

$$3C_3H_8O_3 + 7Fe_2O_3 \leftrightarrow Fe + 12H_2O + 9CO_2 \quad (15)$$

- Steam reactor:

$$3Fe + 4H_2O \rightarrow Fe_3O_4 + 4H_2 \quad (16)$$

- Air reactor:

$$4Fe_3O_4 + O_2 \rightarrow 6Fe_2O_3 \quad (17)$$

3.3 Hydrogen based power generation using bioglycerol as raw-material: conceptual design

The case studies presented in the previous section were modelled and simulated using CHEMCAD software. Simulations of various plant designs for power generation based on hydrogen

production from bioglycerol conversion yield all necessary process data (temperatures, pressures, mass and molar flows, compositions, power generated and consumed) that are needed to assess the overall performance of the processes [8]. Reforming to the chemical looping case, it has to be mentioned that, significant scale-up issues has to be solved before this technology become commercial at the evaluated gas turbine with 334 MW scale. For hydrogen and power generation scenario based on bioglycerol reforming, one M701G2 gas turbine (Mitsubishi Hitachi Power Systems) was used [8, 25-29].

3.4 Dynamic simulation of hydrogen production from bioglycerol steam reforming in a continuous flow tubular reactor

To produce hydrogen or other combustible gasses (e.g. syngas), the glycerol pyrolysis or gasification has received considerable attention [30]. The thermal decomposition of glycerol at high temperatures had CO, H_2, CO_2, CH_4 and C_2H_4 as main products [31]. The major drawback of glycerol pyrolysis is carbon formation due to the cracking of some hydrocarbons including CH_4 [32]. A considerable number of researchers have been investigated the steam reformation of oxygenated hydrocarbons. In last year's Yang et al. had performed a thermodynamic analysis of glycerol steam reforming for hydrogen production, the results showed that higher carbon-oxygen ratio and steam-carbon ratio favor the production of hydrogen [30,33].

Hydrogen production by catalytic glycerol steam reforming can occur first through glycerol dehydrogenation onto the catalyst surface and undergo desorption, followed by the water gas shift or the methanation reaction.The reforming process takes place under the action of a metal catalyst capable of breaking C-C bonds into smaller molecules (e.g. CH_4, CO_2, CO, H_2O, C_2H_4O) [34]. Most studies for hydrogen production from glycerol, published in the literature, were mainly focused on noble metal-based catalysts and commercially available catalysts with low cost. To make using of glycerol in H_2 production process more sustainable, a low-cost catalyst is recommended: Ni–Mg–Al, Ni–Cu–Al, Ni–Cu–Mg, Ni–Mg, Ni–Al catalysts. From kinetics mechanism point of view, hydrogen may be produced from various carbohydrates employing aqueous phase reforming. The reaction pathway for bio-glycerol steam reforming, in the case of 10% Ni - Al_2O_3 as a catalyst, published by Guo et al., is used in this work [35].

The following reaction pathway was used for kinetic parameter analysing [35-37]:

- The glycerol pyrolysis:

(R_1) $C_3H_8O_3 \rightarrow INT + CO_2 + 2H_2$, $R1 = K_1 * C_{C3H8O3}$ (18)

(R_2) $C_3H_8O_3 \rightarrow INT + CO + H_2 + H_2O$, $R2 = K_2 * C_{C3H8O3}$ (19)

- The intermediate component steam reforming:

(R_3 $INT + H_2O \rightarrow 2CO + 3H_2$, $R3 = K_3 * C_{INT} * C_{H2O}$ (20)

(R_4) $INT + 3H_2O \rightarrow 2CO_2 + 5H_2$, $R4 = K_4 * C_{INT} * C_{H2O}$ (21)

- The intermediate component pyrolysis:

(R_5) $INT \rightarrow CO + CH_4$, $R5 = K_5 * C_{INT}$ (22)

- Water-Gas Shift reaction (WGSR):

(R_6) $CO + H_2O \rightarrow CO_2 + H_2$, $R6 = K_6 * C_{CO} * C_{H2O}$ (23)

- The methanation process:

(R_7) $CO + 3H_2 \leftrightarrow CH_4 + H_2O$, $R7 = K_7 * C_{CO} * C_{H2}$ (24)

The hydrogen production based on bio-glycerol steam reforming in a continuous flow tubular reactor is presented in Figure 3-0-1. The first section of the tubular reactor is used to pre-heat the glycerol solution at the reaction temperature. The second section of the tubular reactor is the catalyst layer. The third section of the reactor is for the gas product cooling.

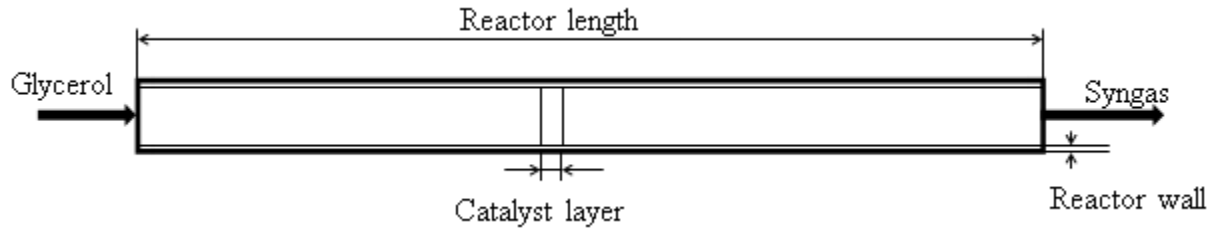

Figure 3-0-1 Tubular reactor for bio-glycerol steam reforming

The effects of operating parameters (temperature, residence time, etc.) and catalyst types, on steam reforming of glycerol were experimentally systematical studied [38], and the results showed that the steam reforming of glycerol for hydrogen production has good prospects. The multitude of reaction intermediaries that are generated in different conditions gives a complex kinetic model. Due to the complexity of the mathematical model, given by the multitude of variables that influence hydrogen production, the processes of steam reforming of bioglycerol with hydrogen generation is less studied in the literature [39-42].

From the dynamic point of view, the system behaves like an element with a large time constant and delay. The dynamic mathematical model can be used to analyze and understand the interaction of various processes that take place inside the reforming reactor and also to make the preliminary calculation of experimental parameters. This paper aims to develop a dynamic model of bio-glycerol steam reforming process in a tubular catalytic reactor.

Reference (summary):

1. C.C. Cormos, A. Imre-Lucaci, A.M. Cormos, Zs. Tasnadi-Asztalos, M. D. Lazar, *Computer Aided Chemical Engineering*, **2013**, 32, 19.
2. Zs. Tasnadi-Asztalos, A. Imre-Lucaci, C.-C. Cormos, A.-M. Cormos, M.-D. Lazar, P.-S. Agachi; *Proceedings of the 24th European Symposium on Computer Aided Process Engineering – ESCAPE 24 June 15-18*, **2014**, Budapest, Hungary
3. S. Adhikari, S. Fernando, S.R. Gwaltney, S.D. Filip To, R.M. Bricka, P.H. Steele, A. Haryanto, *Int J Hydrogen Energy*, **2007**, 32, 2875.
4. F. Díaz Alvarado, F. Gracia, *Int J Hydrogen Energy*, **2012,** 37, 14820.
5. D. Castello, L. Fiori, *Bioresource Technol*, **2011**, 102, 7574.
6. T. Pairojpiriyakul, W. Kiatkittipong, W. Wiyaratn, A. Soottitantawat, A. Arpornwichanop, N. Laosiripojana, E. Croiset, S. Assabumrungrat, *Int J Hydrogen Energy*, **2010,** 35, 10257.
7. Y. Li, W. Wang, B. Chen, Y. Cao, *Int J Hydrogen Energy*, **2010,** 35, 7768.
8. Zs. Tasnadi-Asztalos, P.-S. Agachi, C.-C. Cormos; *International Journal of Hydrogen Energy*, **2015**, 40, 22, 7017
9. European Commission. Energy roadmap 2050. COM(2011) 885/2. **2011**. Brussels, Belgium.

10. Zs .Tasnadi-Asztalos, A. Imre-Lucaci, C.C. Cormos, A.M. Cormos, M.D. Lazar, P.S. Agachi, *Comput Aided Chem Eng*, **2014,** 33, 1735.
11. K. Liu, C. Song, V. Subramani, Hydrogen and syngas production and purification technologies. Hoboken, New Jersey, USA: AIChE-Wiley, John Wiley & Sons Inc.; **2010**.
12. International Energy Agency - Greenhouse Gas R&D Programme (IEA-GHG). Co-production of hydrogen and electricity by coal gasification with CO_2 capture. 2007. Report 13/**2007**.
13. R.M. Navarro, M.A. Pena, J.L.G. Fierro, *Chem Rev*, **2007**, 107, 3952.
14. J.M. Silva, M.A. Soria, L.M. Madeira, *Renew Sust Energy Rev*, **2015**, 42, 1187.
15. Cormos CC. *Int J Hydrog Energy*, **2014**, 39, 5597.
16. A. Blasi, G. Fiorenza, C. Freda, V. Calabr_o, Steam reforming of biofuels for the production of hydrogen-rich gas. In: Gugliuzza A, Basile A, editors. Membranes for clean and renewable power applications. Woodhead Publishing Limited; **2014**, 145.
17. A. Kohl, R. Nielsen, Gas purification. 5th ed. Huston: Gulf Publishing Company; **1997**.
18. P. Padurean, C.C. Cormos, P.S .Agachi, *Int J Greenh Gas Con*, **2011**, 7, 1.
19. C.C. Cormos, A.M. Cormos, S. Agachi, *Asia Pac J Chem Eng*, **2009,** 4, 870.
20. J. Adanez, A. Abad, F. Garcia-Labiano, P. Gayan, L. de Diego, *Prog Energy Combust*, **2012**, 38, 215.
21. B. Dou, Y. Song, C. Wang, H. Chen, M. Yang, Y. Xu, *Appl Energy*, **2014,** 130, 342.
22. P. Chiesa, G. Lozza, A. Malandrino, M. Romano, V. Picollo, *Int J Hydrog Energy*, **2008,** 33, 2233.
23. C.C. Cormos, *Int J Hydrog Energy*, **2010**, 35, 2278.
24. S. Shao, A.W. Shi, C.L. Liu, R. Yang, W.S. Dong, *Fuel Process Technol*, **2014**, 125, 1.
25. A. M. Ribeiro, C. A. Grande, F. V. S. Lopes, J. M. Loureiro, A. E. Rodrigues, *Chem Eng Sci*, **2008,** 63, 5258.
26. V. G. Gomes, K. W. K. Yee, *Sep Purif Technol* , **2002**, 28**,** 161
27. Mitsubishi Heavy Industries. MHI Gas Turbine Technology**.** www.mhi-global.com (accessed 15.06.2015)
28. T. Methling, N. Armbrust, T. Haitz, M. Speidel, N. Poboss, M. Braun-Unkhoff, H. Dieter, B. Kempter-Regel, G. Kraaij, U. Schliessmann, Y. Sterr, A. Wörner, T. Hirth, U. Riedel, G. Scheffknecht, *Bioresource Technol*, **2014,** 169, 510
29. A. Thakur, C. E. Canter, A. Kumar, *App Energ*, **2014,** 128**,** 246
30. B. Dou, Y. Song, C. Wang, H. Chen, Y. Xu, *Renewable Sustainable Energy Rev*., **2014**, 30, 950.
31. K.C. Chin, Y.F. Say, A.A. Adesoji, *Catal. Today*, **2011**, 178, 25.
32. T. Valliyappan, N. N. Bakhshi, A. K. Dalai, *Bioresour. Technol*., **2008**, 99, 4476.
33. G. X. Yang, H. Yu, F. Peng, H. J. Wang, J. Yang, D. L. Xie, *Renewable Energy*, **2011**, 36, 2120.
34. Zs. Tasnadi-Asztalos, A. Imre-Lucaci, A.M. Cormos, D.M. Lazar, P.S. Agachi, *Studia Univ. Babes-Bolyai*, **2013**, 58, 101.
35. S. Guo, L. Guo, J. Yin, H. Jin, *J. of Supercrit Fluid*, **2013**, 78, 95.
36. F. Pompeo, G. Santori, N. N. Nichio, *Int. J.HydrogenEnerg*., **2010**, 35, 8912.

37. V. Nichelea, M. Signorettoa, F. Menegazzoa, A. Gallob, V. D. Santoc, G. Crucianid, G. Cerratoe, *App.Catal., B* **2012,** 111-112, 225.
38. S. Guo, L. Guo, C. Cao, J. Yin, Y. Lu, X. Zhang, *Int. J. of Hydrogen Energ*., **2012**, 37, 5559.
39. A. Sushil, D. F. Sandun, H. Agus, *Chem. Eng. Technol.*, **2009**, 32, 541.
40. R. Sundari and P. D. Vaidya, *Energy Fuels*, **2012**, 26, 4195.
41. A. Sushil, D. F. Sandun, F. S. D. To, M. R. Bricka, P. H. Steele and H. Agus, *Energy & Fuels*, **2008,** 22, 1220.
42. K. C. Chin, Y. F. Say, A. A. Adesoji, *Catal.Commun*., **2010**, 12, 292.

Part II – Hydrogen production and hydrogen based power generation from bioethanol

Chapter 4. Hydrogen production with steam reforming of bioethanol

4.2. Thermodynamic analysis of steam reforming of ethanol

The goal of the thermodynamic analysis is to determine the conditions favorable to maximize the concentration of H_2 and to reduce to as low as possible the concentration of unwanted byproducts as: CH_4, CO_2 and CO. The thermodynamic study was performed using CHEMCAD process simulator. The equilibrium composition was determined for all possible combinations of the following values of parameters *T*, *p* and *r*:

- *T:* 100, 150, 200, 250, 300, 350, 400, 450, 500, 550, 600, 650, 700, 750, 800, 850, 900, 950 and 1000°C;
- *p:* 1, 3, 5, 7, 9, 11, 13, 15, 17, 19, 21, 23, 25, 27, 29 and 30 bar;
- *r:* 3, 5, 7, 9, 11, 13, 15, 17, 19, 21, 23 and 25.

In Figure 4-0-1 are presented in 3D the concentration variations of hydrogen) b) carbon monoxide c) carbon dioxide d) methane depending on pressure and temperature at an initial water:ethanol molar ratio: 25:1. In Figure 4-0-1-a it can be seen as the most favorable condition for the formation of hydrogen is at atmospheric pressure and temperature in the range of 600-700°C. Variation of the concentration of carbon monoxide in function of the temperature and pressure at water:ethanol molar ratio 25:1 is presented in Figure 4-0-1-b. The maximum concentration of carbon monoxide (8 mol%) is reached at 1000°C and is independent of pressure. In Figure 4-0-1-c is presented to the carbon dioxide concentration variation depending on the pressure and temperature at water:ethanol molar ratio 25:1. The concentration of carbon dioxide in the case of the most favorable hydrogen formation is in the range 23-23.5% mol. Variation of the concentration of methane, depending on the temperature and pressure for a water:ethanol molar ratio 25:1 is presented in Figure 4-0-1-d. It can be seen as the most unfavorable condition of steam reforming of ethanol for methane (0% mol) is at elevated temperatures (1000°C) and at atmospheric pressure.

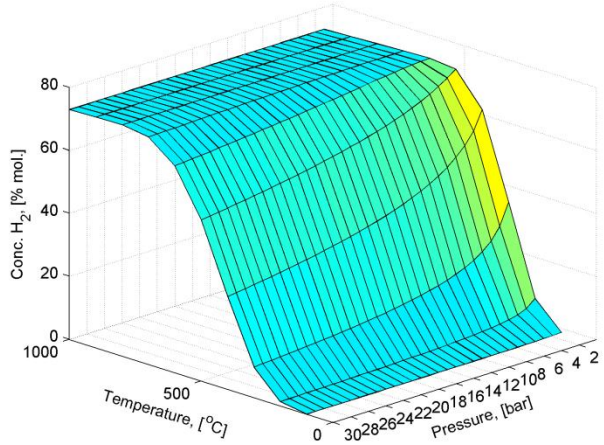

a)

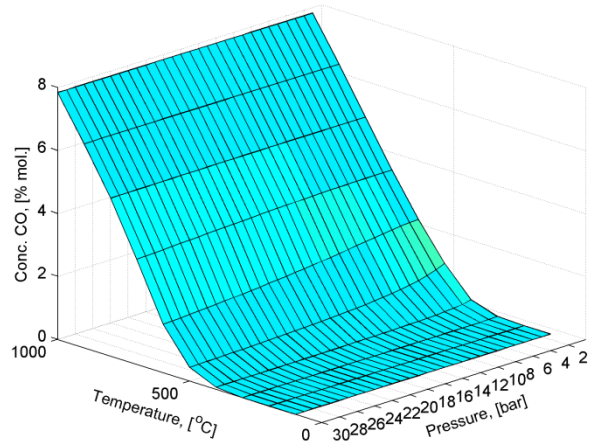

b)

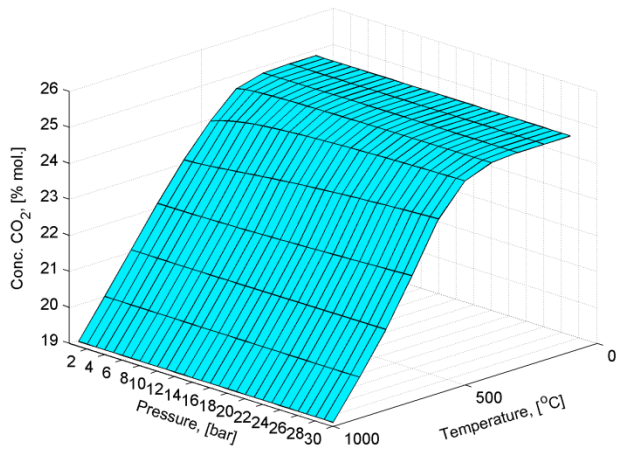

c)

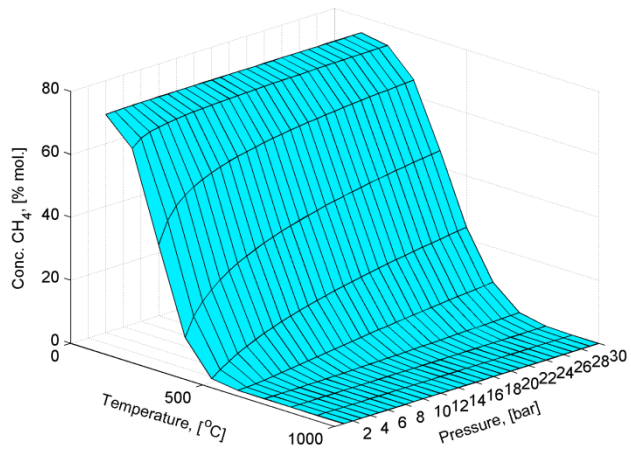

d)

Figure 4-0-1 Variation of main components concentration for a water:ethanol molar ratio 25:1 a)H_2 b)CO c)CO_2 d)CH_4

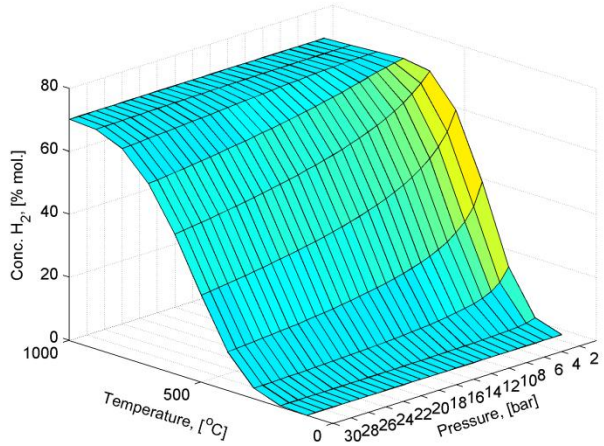

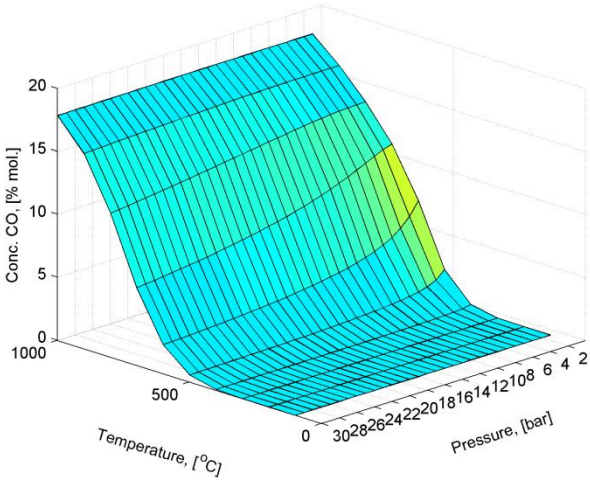

a) b)

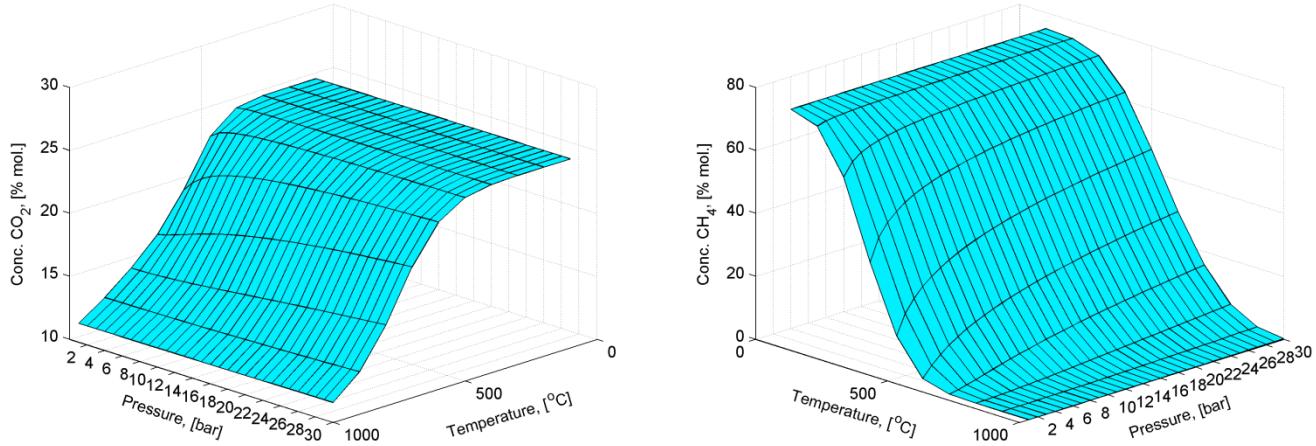

c) d)

Figure 4-0-2 Variation of main components concentration for a water:ethanol molar ratio 7:1 a)H_2 b)CO c)CO_2 d)CH_4

In Figure 4-0-2 are presented the variations of concentration for a) H_2 b) CO) c) CO_2 d) CH_4 depending on pressure and temperature for initial water:ethanol molar ratio 7:1. Four component concentration values represented in figure above serve as a comparison with the values of concentrations from the simulation of the entire technological process of steam reforming of crude ethanol with hydrogen production, as in the simulation of the entire technological process as raw-materials using ethanol derived from biomass fermentation.

4.3. Kinetic studies of steam reforming of ethanol

There are few papers in the literature on kinetic studies of ethanol steam reforming, because the system complexity. Ethanol was used as the representative component for bioethanol because of its much higher concentration compared to other components that are present in the bioethanol mixture.
The experimental conditions are presented in Table 4-1.

Table 4-1 Main experimental parameters

Parameters	U.M.	Values
$F_{V,T}$	[mL/min]	10.1, 35.1, 133.1, 200.1, 300.1
$F_{V,dry}$	[mL/min]	0.1
W	[g]	1
T	[C]	350
$Time$	[h]	24
P	[bar]	3
D	[mm]	8
Dp	[μm]	88

Argon was used as carrier gas. Experiments were performed at five different Ar flows (10, 35, 133, 200, 300 mL/min) in order to have a set of space time ($\theta_V = W/F_{V,T}$) values, a parameter that influences the reaction rate.

The four kinetic parameters were recalculated by minimizing the objective function that describes the relative deviations between experimental and calculated concentration date on the set of 5 different experimental sets as follows:

$$fob = \sum_{i\to 5}^{Exp}\left[\left(\frac{y_{exp}-y_{calc}}{y_{calc}}\right)^2\right] \overset{!}{=} \min \qquad (1)$$

The calculated values of the four kinetic model parameters are presented in Table 4-2.

Table 4-2 Global kinetic constants of SRE.

Parameter	Calculated values
k_{E1sim}	$3.64\cdot10^{-5}$
k_{E2sim}	$1.44\cdot10^{-5}$
k_{R1sim}	$0.55\cdot10^{-3}$
k_{R2sim}	$4.33\cdot10^{-2}$

Using these recalculated values, the variations of the main components concentrations obtained from the adjusted kinetic model are presented in Figure 4-3.

The kinetic model was implemented in MATLAB.

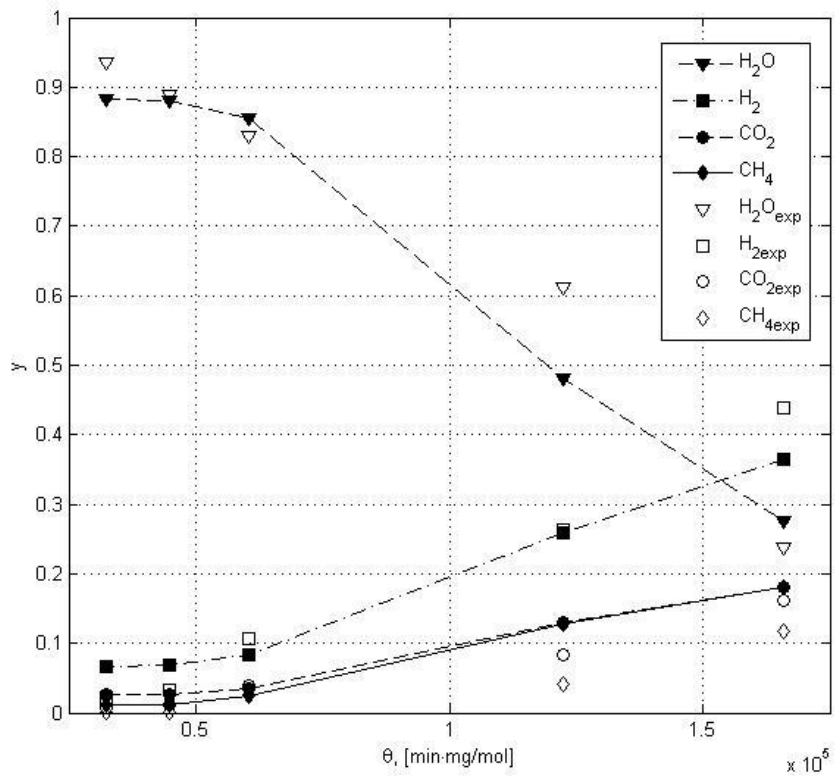

Figure 4-3 Measured and simulation data of steam reforming of bioethanol (with symbols are shown the experimental data and with lines and symbols the simulation results)

Chapter 5. Hydrogen based power generation from ethanol

5.2. 300 MW_{th} Hydrogen production from ethanol reforming

The following hydrogen production concepts were investigated in this subchapter:

Case 1a: Hydrogen production from crude ethanol steam reforming without carbon capture and storage;

Case 1b: Hydrogen production from crude ethanol steam reforming with carbon capture and storage;

Case 2a: Hydrogen production from crude ethanol autothermal reforming with O_2 without carbon capture and storage;

Case 2b: Hydrogen production from crude ethanol autothermal reforming with O_2 with carbon capture and storage;

Case 3a: Hydrogen production from crude ethanol autothermal reforming with air without carbon capture and storage;

Case 3b: Hydrogen production from crude ethanol autothermal reforming with air with carbon capture and storage;

Case 4: Hydrogen production by direct ethanol chemical looping conversion.

All evaluated plant options were designed to produce 300 MW_{th} hydrogen based on lower heating value (10.8 MJ/Nm^3), this corresponds to 100,000 Nm^3/h, with almost null net power output.

The power generated within the plant is mainly used for covering the ancillary consumption; this is also the case for the steam generated in the plant [1].

The fuel used in this analysis is the crude ethanol residues from biomass fermentation. The fuel composition is the following (% wt.): 74.14% ethanol and 25.85% water. Ilmenite ($FeTiO_3$) was used as oxygen carrier for chemical looping Case 4 [2]. The main design characteristics of various plant sub-systems are presented in Table 5-0-1 [3-7]. The case studies presented in this subchapter were modeled and simulated using CHEMCAD software [8].

Table 5-0-1 Main plant design characteristics

Bio-fuel served and preheating	Fuel composition: bioethanol solution in water (as resulted from fermentation) Bio-fuel preheating: 400-500 ^{o}C (using hot flue gases from the plant)
Steam Reformer	Thermal mode: heat exchanger or autothermal Pressure: 30 bar; Pressure drop: 1 bar; Outlet temperature: 850 ^{o}C; Ni-based catalyst
Heat exchangers	Pressure drop: 1 % of inlet pressure ΔT_{min}= 10 ^{o}C
Heat recovery steam generation	Three steam pressure levels: low, middle and high Steam turbine isoentropic efficiency: 85 %
Pressure Swing Adsorption (PSA)	Purified hydrogen: > 99.95 % (vol.) Tail gas pressure: 1.5 bar; Purification yield: 65–85 %
Carbon capture unit (Cases 1b, 2b and 3b)	Solvent regeneration: thermal Solvent: Methyl-di-ethanol-amine (MDEA) Absorption: desorption cycle
Carbon capture unit (Case 4)	Oxygen carrier: ilmenite Fuel reactor parameters: 28 bar/ 700 ^{o}C Steam reactor parameters: 26 bar/ 715 ^{o}C Air reactor parameters: 24 bar/ 985 ^{o}C Thermal mode: adiabatic
CO_2 compression and drying	Delivery pressure: 120 bar; Compressor efficiency: 85 % 4 compression stages with intercooling Captured CO_2 quality specification (%vol.): CO_2 >95 %; CO<2000 ppm; H_2O<250 ppm; H_2S<100 ppm; other gases <4 %
Tail gas expander	Expander efficiency: 70 %; Tail gas preheating before expansion: 230 ^{o}C;

	Outlet pressure: 1.5 bar

The definitions of the key performance indicators, used in the comparison of various cases, are presented in the next section.

Hydrogen efficiency (η_{H_2}) of ethanol reforming is calculates as follows:

$$\eta_{H_2} = \frac{hydrogen\ thermal\ energy\ [MW]}{ethanol\ thermal\ energy\ [MW]} * 100 \quad (1)$$

Net electrical efficiency (η_{net}) of ethanol reforming shows overall plant performance in term of electricity conversion process, they are calculated with the formula:

$$\eta_{net} = \frac{net\ power\ output\ [MW]}{ethanol\ thermal\ energy\ [MW]} * 100 \quad (2)$$

Cumulative efficiency ($\eta_{cumulative}$) of ethanol reforming is calculated by adding net electrical efficiency and hydrogen efficiency:

$$\eta_{cumulative} = \eta_{net} + \eta_{H_2} \quad (3)$$

Carbon capture rate (CCR) of ethanol reforming is calculated considering the molar flow of captured carbon dioxide divided by carbon molar flow from the feedstock (crude ethanol):

$$CCR = \frac{captured\ CO_2\ molar\ flow\ [kmole/h]}{ethanol\ carbon\ molar\ flow\ [kmole/h]} * 100 \quad (4)$$

Specific CO_2 emission (SE_{CO_2}) of ethanol reforming is calculated considering the emitted CO_2 mass flow for each MW of hydrogen and power co-generated:

$$SE_{CO_2} = \frac{emitted\ CO_2\ mass\ flow\ [kg/h]}{net\ power\ output\ [MW] + hydrogen\ energy\ [MW]} \quad (5)$$

Table 5-0-2 presents the overall technical plant performance indicators for the hydrogen production designs based on bioethanol steam, autothermal reforming with and without carbon capture and direct chemical looping.

Table 5-0-2 Overall technical plant performance indicators

Main plant data	Units	Case 1a	Case 1b	Case 2a	Case 2b	Case 3a	Case 3b	Case 4
Crude ethanol flow rate	t/h	241.19	241.19	274.45	274.45	274.43	274.43	244.34
Ethanol lower heating value (LHV)	MJ/kg	28.86	28.86	28.86	28.86	28.86	28.86	28.86
Feedstock thermal energy-LHV(A)	MW_{th}	500.02	500.02	568.96	568.96	568.92	568.92	506.55
Steam turbine output	MW_e	37.92	49.14	16.95	16.15	18.13	18.70	19.31
Expander power output	MW_e	2.47	1.24	2.73	1.07	5.60	3.89	102.19
Gross electric power output(B)	MW_e	40.39	50.39	19.68	17.22	23.73	22.59	121.51

ASU power consumption	MW_e	0	0	11.21	7.83	0	0	0
Reformer island power consumption	MW_e	0.27	0.27	0.31	3.32	14.87	14.87	77.72
Carbon capture + CO_2 drying and compression	MW_e	0	6.96	0	8.49	0	8.68	2.51
Power island power consumption	MW_e	0.30	0.57	0.14	0.13	0.16	0.17	0.11
Hydrogen compression	MW_e	3.88	3.91	3.85	4.03	3.85	4.06	2.07
Total ancillary power consumption (C)	MW_e	4.41	11.72	15.52	23.83	18.89	27.79	82.44
Hydrogen output (D)	MW_{th}	300	300	300	300	300	300	300
Net electric power output (E=B-C)	MW_e	35.97	38.66	4.16	-6.60	4.83	5.19	39.07
Net hydrogen efficiency (D/A * 100)	%	59.99	59.99	52.72	52.72	52.73	52.73	59.22
Net electrical efficiency (E/A*100)	%	7.19	7.73	0.73	-1.16	0.85	-0.91	7.71
Cumulative energy efficiency	%	67.18	67.72	53.45	51.55	53.58	51.81	66.93
Carbon capture rate	%	0	85.04	0	88.95	0	90.91	93.54
Specific CO_2 emissions (hydrogen and power)	Kg/MWh	354.63	63.52	445.73	44.41	444.72	32.95	1.79

In this section of the subchapter various options for carbon capture (MDEA-based gas-liqiud absorption, syngas-based on chemical looping), were evaluated and compared, the most promising being the chemical looping technology. The chemical looping concept presents comparable cumulative energy

efficiency with steam reforming without carbon capture concept. Case 4 have higher carbon capture rate than Case 3b (with >2.6%). In the case of specific CO_2 emissions the chemical looping option has the lowest value.

The captured carbon dioxide quality specification is important in any plant equipped with carbon capture. The specification of captured CO_2 stream has to be in line with the transport and storage requirements. This thesis is using the most limiting storage option (namely Enhanced Oil Recovery - EOR). The content of CO_2 in the CO_2 captured stream has to be at least 95% (vol.) [9-11]. In each evaluated carbon capture case, quality specification of captured CO_2 stream was calculated .

5.3. Pinch analysis for hydrogen production at industrial scale from crude ethanol

This section presents results of PINCH analysis for hydrogen production at industrial scale for the process of reforming the raw ethanol. These results are obtained by using the MATLAB simulation program. As incoming data (temperature, specific heat, mass flow, mol fraction, etc.) in the simulation analysis of PINCH input streams are used and in heat exchangers from simulations conducted for the entire technological process of reforming the raw ethanol made with CHEMCAD 6.0.1 process simulator described in Chapter 5.2[12-26].

In Figure 5-0-1-a are presented to hot and cold flows temperature ranges of direct chemical looping of crude ethanol. Composite curves for CCS unit of hydrogen production by direct crude ethanol chemical looping conversion with include CO_2 storage is presented in Figure 5-0-1-b. In Figure 5-0-1-b you can see that it not reached PINCH point. In each heat exchanger of Case 4 does not touch the PINCH point and a minimum temperature of 5ºC between the temperature of the exhaust flow hot and cold streams.

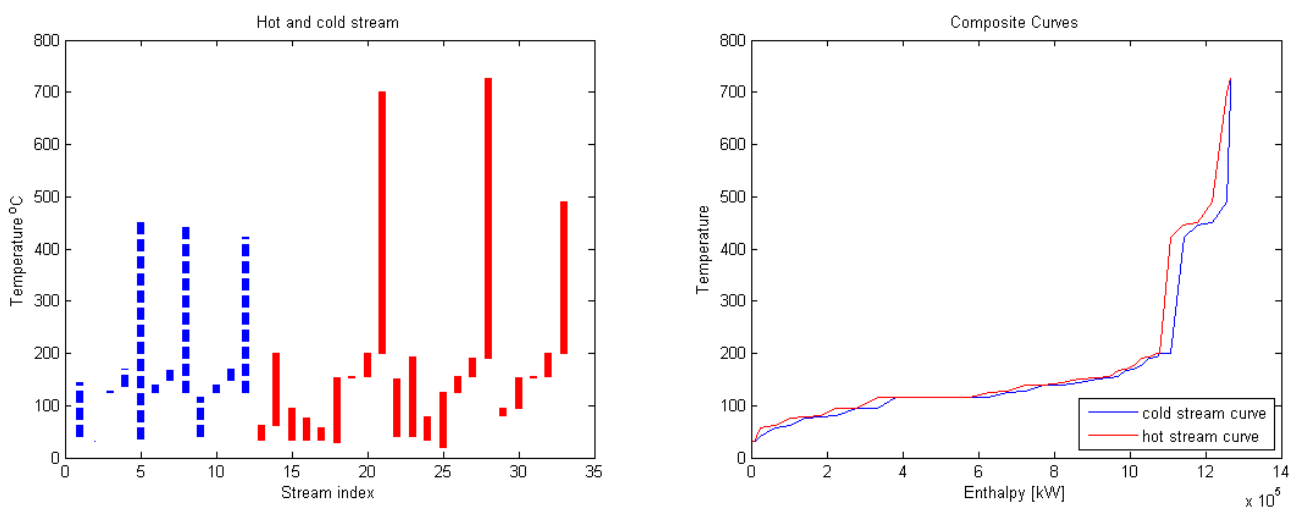

a) b)

Figure 5-0-1 Ethanol direct chemical looping to hydrogen production (equivalent 300MW$_{th}$)

5.4. Hydrogen-based power generation using bioethanol as raw-material: conceptual design

The following hydrogen-based power generation from crude ethanol reforming concepts was investigated in this subchapter:

Case 1a: Hydrogen-based power generation from crude ethanol steam reforming without carbon capture;

Case 1b: Hydrogen-based power generation from crude ethanol steam reforming with carbon capture.
Case 2a: Hydrogen-based power generation from crude ethanol autothermal reforming with O_2 and without carbon capture;
Case 2b: Hydrogen-based power generation from crude ethanol autothermal reforming with O_2 and with carbon capture.
Case 3a: Hydrogen-based power generation from crude ethanol autothermal reforming with air and without carbon capture;
Case 3b: Hydrogen-based power generation from crude ethanol autothermal reforming with air and with carbon capture.
Case 4: Hydrogen-based power generation by direct crude ethanol chemical looping conversion.

The main design characteristics of various plant sub-systems are presented in Table 5-0-3[3-7]. The case studies presented in this subchapter were modeled and simulated using CHEMCAD software [8].

Table 5-0-3 Main design characteristics for hydrogen-based power generation

Bio-fuel fed and preheating	Fuel composition: 74.14%wt. ethanol; 25.85% wt. water Bio-fuel preheating: 400-500 ^{o}C
Reformer	Ni-based catalyst Pressure: 30 bar Pressure drop: 1 bar Outlet temperature: 850 ^{o}C Thermal mode: heat exchanger and autothermal
Heat exchangers	ΔT_{min}= 10 ^{o}C Pressure drop: 1% of inlet pressure
Heat recovery steam generation	Three steam pressure levels: low, middle and high Steam turbine isoentropic efficiency: 85%
Tail gas expander	Tail gas preheating before expansion: 230 ^{o}C Outlet pressure: 1.5 bar Expander efficiency: 70 %
Pressure Swing Adsorption (PSA)	Purified hydrogen: > 99.95 % (vol.) Purification yield: 65 – 85 % Tail gas pressure: 1.5 bar
CO_2 compression and drying	Delivery pressure: 120 bar 4 compression stages with intercooling Compressor efficiency: 85% Drying solvent: TEG (Tri-ethylene-glycol) Captured CO_2 quality specification (%vol.): CO_2 >95 %; CO <2000 ppm; H_2O <250 ppm; H_2S <100 ppm; other gases <4%
Carbon capture unit (Cases 1b, 2b and 3b)	Solvent: Methyl-diethanol-amine (MDEA)

	Solvent regeneration: thermal Absorption: desorption cycle
Carbon capture unit (Case 4)	Oxygen carrier: ilmenite Fuel reactor parameters: 28 bar/ 700 °C Steam reactor parameters: 26 bar/ 715 °C Air reactor parameters: 24 bar/ 985 °C Thermal mode: adiabatic

The definitions of the key performance indicators, used in the comparison of various cases, are presented in the next section.

Net electrical efficiency (η_{net}) of hydrogen-based power generation from crude ethanol shows overall plant performance in term of electricity conversion process, they are calculated with the formula:

$$\eta_{net} = \frac{net\ power\ output\ [MW]}{ethanol\ thermal\ energy\ [MW]} * 100 \quad (6)$$

Carbon capture rate (CCR) of hydrogen-based power generation from crude ethanol is calculated considering the molar flow of captured carbon dioxide divided by carbon molar flow from the feedsotck (crude ethanol):

$$CCR = \frac{captured\ CO_2\ molar\ flow\ [kmole/h]}{crude\ ethanol\ carbon\ molar\ flow\ [kmole/h]} * 100 \quad (7)$$

Specific CO_2 emission (SE_{CO_2}) of hydrogen-based power generation from crude ethanol is calculated considering the emitted CO_2 mass flow for each MW of hydrogen and power co-generated:

$$SE_{CO_2} = \frac{emitted\ CO_2\ mass\ flow\ [kg/h]}{net\ power\ output\ [MW] + gas\ turbine\ [MW]} \quad (8)$$

Table 5-0-4 presents the overall technical plant performance indicators for the hydrogen-based power generation designs based on bioethanol steam, autothermal reforming with and without carbon capture and bioethanol direct chemical looping.

Table 5-0-4 Overall technical plant performance indicators

Main plant data	Units	Case 1a	Case 1b	Case 2a	Case 2b	Case 3a	Case 3b	Case 4
Crude ethanol flowrate	t/h	170.05	170.05	193.50	193.50	193.50	193.50	172.27
Crude ethanol LHV	MJ/kg	28.86	28.86	28.86	28.86	28.86	28.86	28.86
Feedstock thermal energy-LHV(A)	MW_{th}	1363.51	1363.51	1551.51	1551.51	1551.51	1551.51	1381.28
Steam turbine output	MW_e	176.02	168.56	223.34	211.81	237.61	211.12	216.72
Expander power output	MW_e	7.16	3.86	8.02	3.36	15.72	10.94	332.80
Gas turbine	MW_e	334	334	334	334	334	334	334

Gross electric power output(B)	MW_e	517.18	506.43	565.36	549.18	587.33	556.07	883.52
ASU power consumption	MW_e	0	0	29.57	29.57	0	0	0
Reformer island power consumption	MW_e	0.75	0.75	0.86	0.86	40.55	40.55	247.63
Carbon capture + CO_2 drying and compression	MW_e	0	17.57	0	22.59	0	23.01	6.86
Power island power consumption	MW_e	2.53	2.53	2.77	3.13	2.78	2.77	2.68
Hydrogen compression	MW_e	0	0	0	0	0	0	5.67
N_2 compression	MW_e	19.46	19.46	19.46	19.46	19.46	19.46	19.46
Total ancillary power consumption (C)	MW_e	22.76	40.32	52.67	75.63	62.81	85.81	282.31
Net electric power output (D=B-C)	MW_e	494.42	466.10	512.69	473.54	524.52	470.25	601.20
Net electrical efficiency (D/A*100)	%	36.26	34.18	33.04	30.52	33.80	30.30	43.52
Carbon capture rate	%	0	78.26	0	88.04	0	89.68	93.82
Specific CO_2 emissions (power)	Kg/MWh	659.62	128.49	723.49	59.40	707.18	45.54	35.83

The chemical looping concept presents comparable cumulative energy efficiency with steam reforming without carbon capture concept. Case 4 have higher carbon capture rate than Case 3b (with >4.1%). In the case of specific CO_2 emissions the chemical looping option has the lowest value.

The captured carbon dioxide quality specification is important in any plant equipped with carbon capture. The specification of captured CO_2 stream has to be in line with the transport and storage

requirements. This thesis is using the most limiting storage option (namely Enhanced Oil Recovery – EOR). The content of CO_2 in the CO_2 captured stream has to be at least 95% (vol.) [10, 11]. In each evaluated carbon capture case, quality specification of captured CO_2 stream was calculated .

5.5. Pinch analysis for hydrogen based power generation from different conceptual design from crude ethanol

This section presents results of PINCH analysis for hydrogen-based power generation at industrial scale for the process of reforming the crude ethanol. These results are obtained by using the MATLAB simulation program.

In Figure 5-0-2-a are presented to hot and cold flows temperature ranges of hydrogen-based power generation with direct chemical looping of crude ethanol. Composite curves for CCS unit of hydrogen-based power generation by direct crude ethanol chemical looping conversion with include CO_2 storage is presented in Figure 5-0-2-b. In Figure 5-0-2-b you can see that it reaches PINCH point around the temperature of 50-60°C. In each heat exchanger of Case 4 does not touch the PINCH point and a minimum temperature of 5ºC between the temperature of the exhaust flow hot and cold streams.

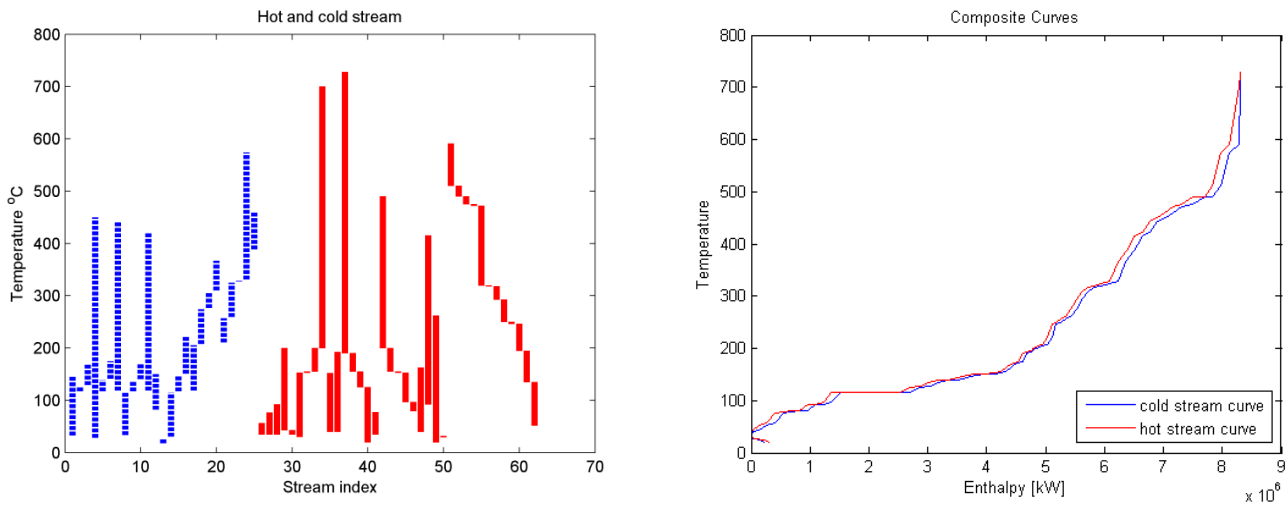

a) b)

Figure 5-0-2 Hydrogen based power generation from chemical looping of ethanol

Reference (summary):

1. Zs. Tasnadi-Asztalos, P.-S. Agachi, C.-C. Cormos; *Int. J. Hydro. Energy*, **2015,** 40, 22, 7017
2. Zs. Tasnadi-Asztalos, A.-M. Cormos, Á. Imre-Lucaci, and C.-C. Cormos; *AIP Conference Proceedings* **2013,** 1565, 175.
3. C.C. Cormos., *Int J Hydrog Energy* **2014**, 39, 5597.
4. K.S. Kang, C.H. Kim, K.K. Bae, W. Cho, S.H. Kim, C.S. Park, *Int J Hydrog Energy* **2010**, 35, 12246.
5. A. Freitas, R. Guirardello, *Int J Hydrog Energy*, 2014, 39, 17969.
6. C. Graschinsky, P. Giunta, N. Amadeo, M. Laborde, *Int J Hydrog Energy* **2012**, 37, 10118.
7. W. Budzianowski, *Int J Hydrog Energy*, **2010**, 35, 7454.

8. ChemCAD. Chemical process simulation e version 6.5. Huston, USA: Chemstations; 2015. www.chemstations.net (accessed 12.02.15.).
9. S. Shao, A.W. Shi, C.L. Liu, R. Yang, W.S. Dong, *Fuel Process Technol*, **2014**, 125, 1.
10. Bade M, Bandyopadhyay S., *Appl Therm Eng*, **2015**, 78, 118.
11. R. Smith, Chemical processes: design and integration. West Sussex, England: Wiley, **2005**.
12. B. Linnhoff, E. Hindmarsh, *Chem. Eng. Sci*. **1983**, 38, 745.
13. A. C. Dimian, C. Bildea, A. Kiss, *Computer Aided Chem. Eng*. **2003**, 13, 393.
14. S. L. W. Alwi, Z. A. Manan, M. Misman, *Proc. of the 11th Int. Symp. on Process System Engineering, Singapore*, **2012**.
15. M. Castier, *Appl. Therm. Eng*. **2007**, 27, 1653.
16. A. I. A. Salama, *Comput. Chem. Eng*. **2005**, 29, 1861.
17. V. Lavric, D. Baetens, V. Plesu, J. D. Ruyck, *Appl. Therm. Eng*. **2003**, 23, 1837.
18. M. G. Bandpy, H. Y. Jelodar, M. Khalili, *Appl. Therm. Eng*. **2011**, 31, 779.
19. A. Martin, F. A. Mato, *Educ. Chem. Eng*. **2008**, 3, 6.
20. M. Bozan, F. Borak, I. Or, *Chem. Eng. Process*. **2001**, 40, 511.
21. A. I. A. Salama, *Comput. Chem. Eng*. **2006**, 30, 758.
22. J. Jezowski, R. Bochenek, A. Jezowska, *Appl. Therm. Eng.* **2000**, 20, 1481.
23. D. M. Fraser, N. Hallale, AIChE J. **2000**, 46, 2112.
24. J. D. Ruyck, V. Lavric, D. Baetens, V. Plesu, *Energy Convers. Manage*., **2003**, 44, 2321.
25. R. Smith, Chemical Process: Design and Integration, Wiley India Edition, New Delhi **2005**.
26. J. M. Douglas, Conceptual Design of Chemical Processes, McGraw-Hill, New York **1998**.

Part III – Hydrogen production and hydrogen based power generation from bioglycerol reforming

6.2. Thermodynamic analysis of catalytic steam reforming of glycerol

Thermodynamics analysis was performed with process CHEMCAD Simulator version 6.0.1. This analysis extends the field of thermodynamics analysis of the main parameters that have the greatest impact on the process of the steam reforming of glycerol (temperature, pressure and molar ratio water-glycerol).

Taking into consideration the results presented in 2D figures were elected as essential conditions for the production of hydrogen via steam reforming of raw glycerol which are presented in Figure 6-0-1 and Figure 6-0-2. Variation of the concentration of H_2, CO, CO_2, respectively CH_4 according to temperature and pressure at an initial water:glycerol molar ratio 10:1 are presented in Figure 6-0-1. In Figure 6-0-1-a can observe that at atmospheric pressure and at 600°C attain maximum concentration of hydrogen. Over this temperature hydrogen concentration has a slight tendency of decrease (less than 1%mol up to 1000°C). The increased pressure at 600°C hydrogen concentration has a tendency of decrease in linear. In Figure 6-0-1-b are presented the variation of carbon monoxide at a initial water:glycerol molar ratio 10:1. From this figure it can be seen as the most favorable condition (low concentration of carbon monoxide) is at 100°C and 1 bar, but at the most favorable condition of formation of hydrogen can be seen a maximum of carbon monoxide. Variation of carbon dioxide

concentration at a molar ratio of water:glycerol 10:1 is presented in Figure 6-0-1-c. It can be seen as a variation of the pressure does not influence the concentration of carbon dioxide. In Figure 6-0-1-d are presented the variation of methane concentration according to temperature and pressure at an initial water:glycerol molar ratio 10:1. From this figure it can be seen as the most favorable condition for methane formation is in the field of temperature 150-250°C, respectively in the field of pressure 10-30bar. Favorable conditions for the formation of hydrogen and methane concentration tends to 0.

Variation of the concentration H_2, CO, CO_2, respectively CH_4 according to pressure and water:glycerol molar ration at 500°C are presented in Figure 6-0-2. In Figure 6-0-2-a it can be seen that the formation of hydrogen is favored at high molar ratios and low pressure. Variation of the concentration of carbon monoxide at 500oC is presented in Figure 6-0-2-b. The formation of carbon monoxide is favored at high pressure and at a water:glycerol molar ratio of 2:1. Favorable conditions for the formation of hydrogen, the carbon monoxide concentration are approximately 26%mol. In Figure 6-0-2-c are presented the variation of carbon dioxide at 500°C. In the most favorable conditions for the formation of hydrogen, the carbon dioxide concentration 1%mol, but the concentration of carbon dioxide is performed at a pressure of 5 bar and at a water:glycerol molar ratio 1:1. Variation of the concentration of methane at 500°C is presented in Figure 6-0-2-d. The most unfavorable condition of formation of methane is the water:glycerol molar ratio 15:1 and at atmospheric pressure (approximately 0.1%mol), but when the hydrogen concentration is maximum, the concentration of methane is 20%mol.

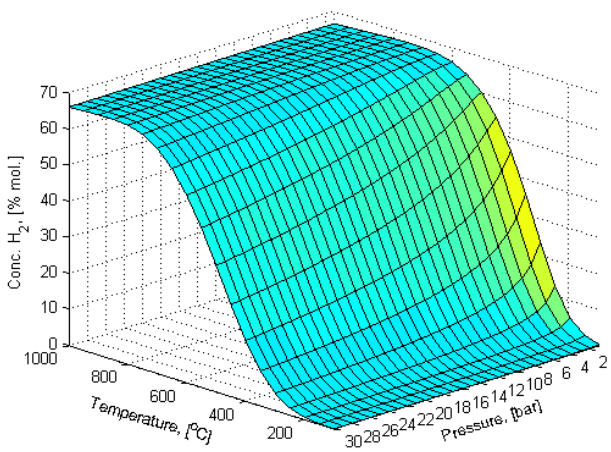

a)

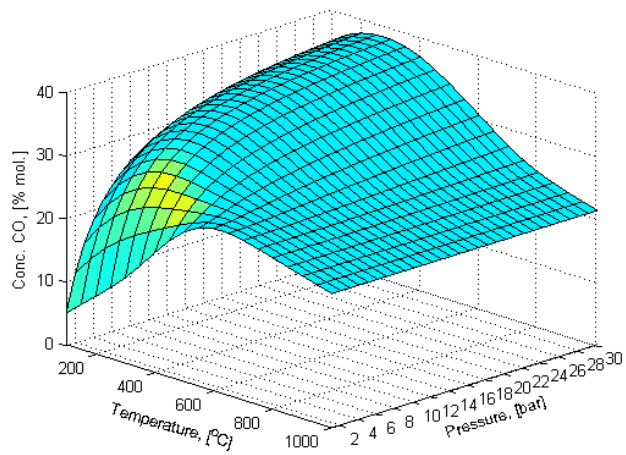

b)

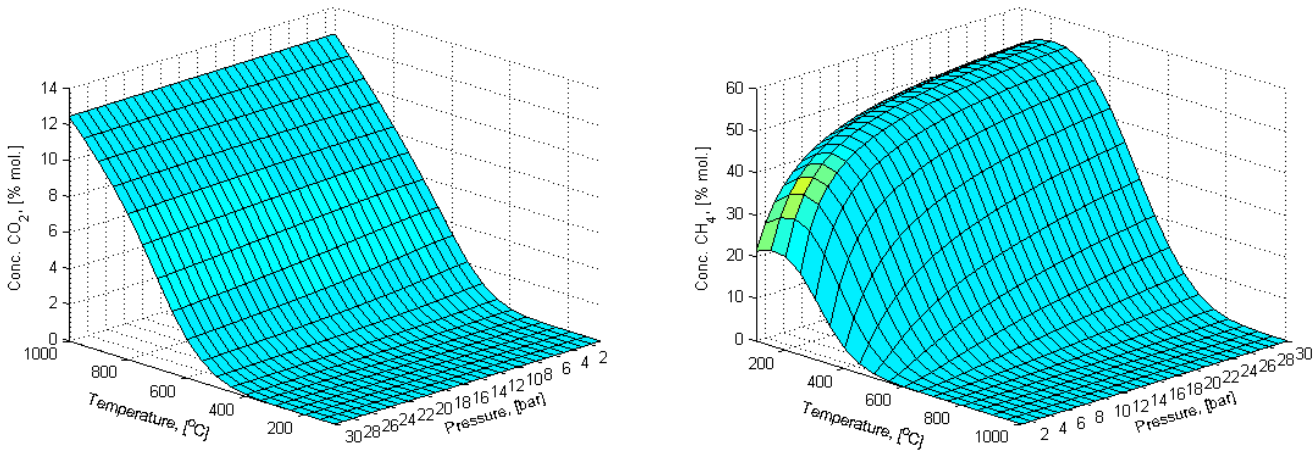

c) d)

Figure 6-0-1 Variation of main components concentration at a water:glycerol molar ratio 10:1: a)H_2 b)CO c)CO_2 d)CH_4

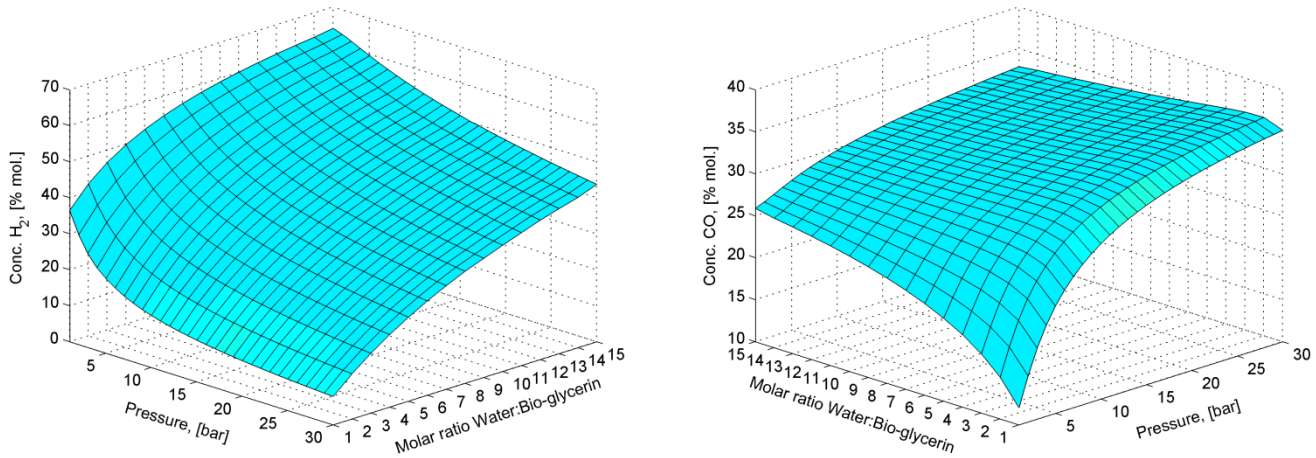

a) b)

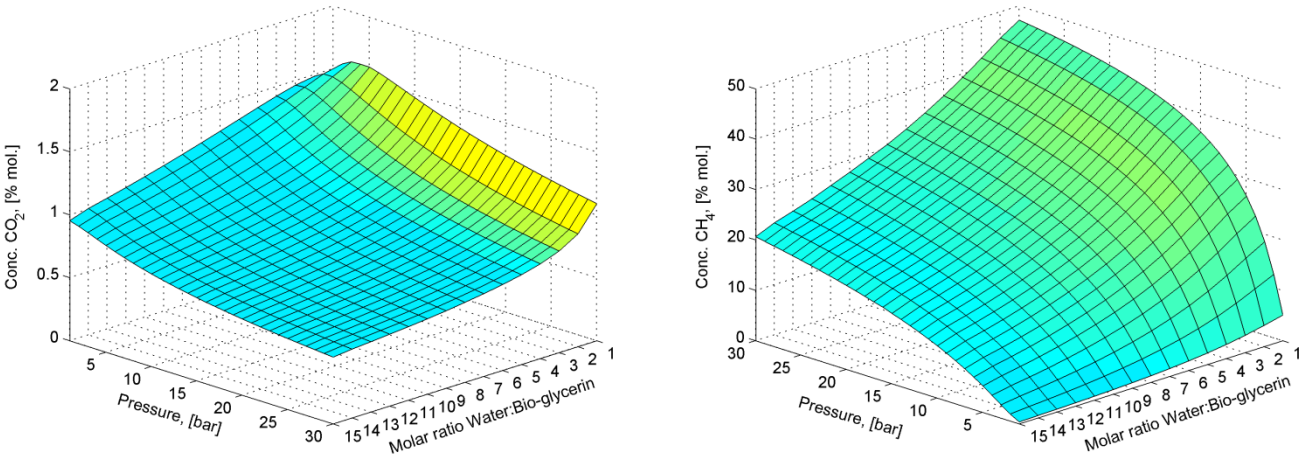

c) d)

Figure 6-0-2 Variation of main components concentration at 500°C: a)H_2 b)CO c)CO_2 d)CH_4

6.3. Dynamic simulation of hydrogen production from bio-glycerol steam reforming in a continuous flow tubular reactor

This subchapter presents the evaluation, done by mathematical modeling and simulation, of hydrogen production based on bioglycerol steam reforming in a catalytic bed reactor to be used in power generation sector. A dynamic mathematical model of crude glycerin conversion into syngas using a nickel-based catalyst was developed and used for analyzing of evolutions of the process parameters and understanding of the micro-level interaction of various processes taking place inside the tubular catalytic reactor. The main model equations are developed by applying the component mass balance equations assuming an ideal plug-flow regime. The mathematical model has been implemented in Matlab/Simulink.

The Figure 6-0-3 shows a zone with a maximum concentration of hydrogen along the catalyst zone between 0.025 - 0.04 m, followed by a slight decrease in the concentration of hydrogen. Increasing the gas flow rate (reported to the nominal value, Q_G = 5Nm^3/h) causes the slowly increase of hydrogen.

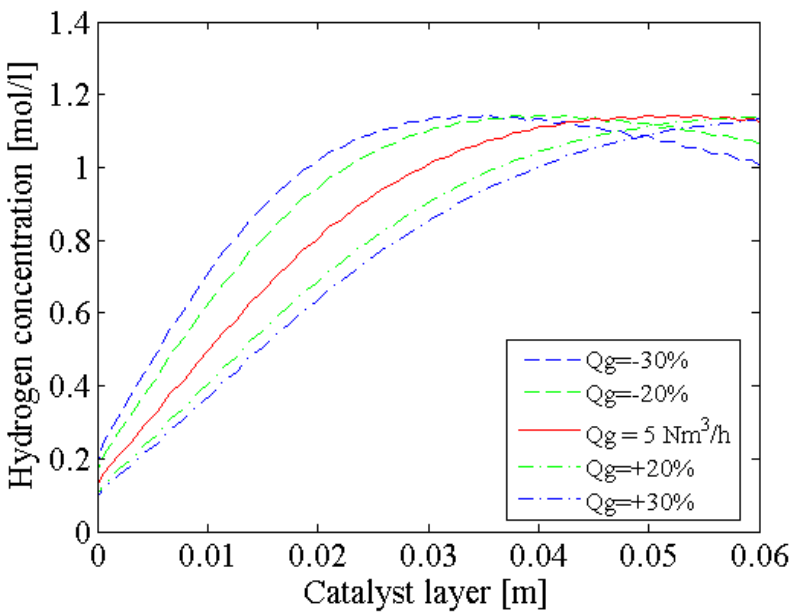

Figure 6-0-3 Hydrogen concentration at 525°C for different flow rates

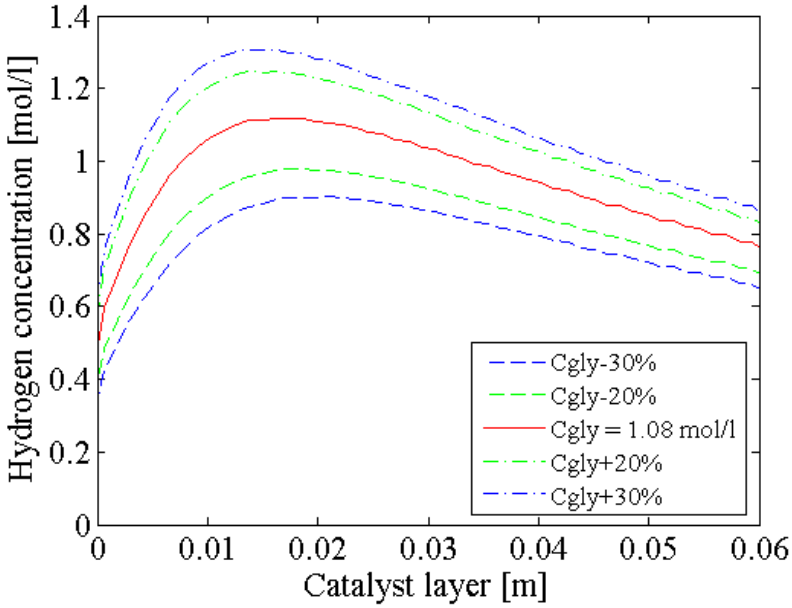

Figure 6-0-4 Hydrogen concentration at 600°C for different initial glycerol concentrations

Figure 6-0-4 presents the hydrogen concentration variation with the catalyst layer for different initial glycerol concentration, at 600°C. In Figure 6-0-4 can be observed if the initial concentration of the glycerol increases, the hydrogen concentration profiles, on the catalyst layer, increases.

The dynamic response of hydrogen concentration for a step decrease of the inlet gas flow with 30%, at 567 °C is presented in Figure 6-0-5. The hydrogen concentration in the catalyst layer is stabilized almost immediately at the new steady-state values, the output hydrogen concentration is 0.75 mol/l.

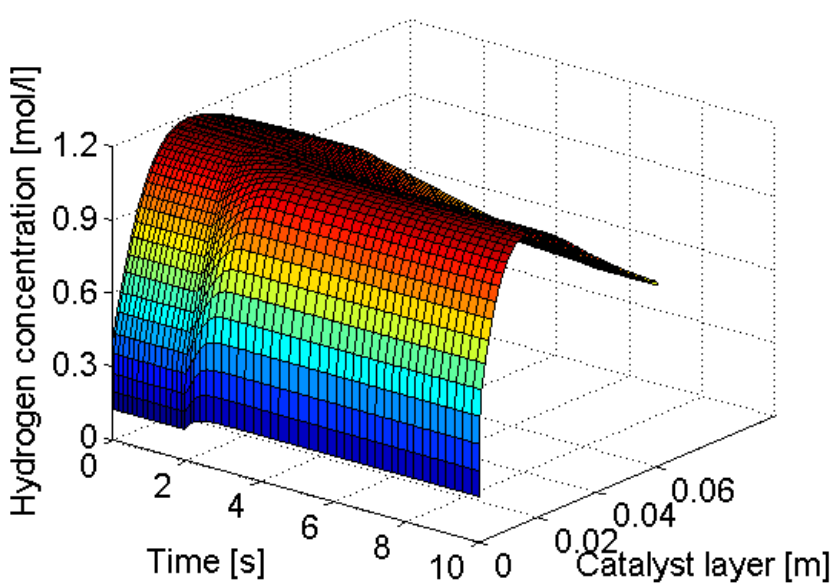

Figure 6-0-5 Dynamic response of hydrogen concentration for a step decrease of ΔQ_G = -30%

Figure 6-0-6 presents the hydrogen concentration, at 567°C, in function of the time and the catalyst layer length when the initial concentration of glycerol is decreased from the nominal value with 30%. The hydrogen concentration profile presents a maximum value in the middle zone of the catalyst layer, followed by a slight decrease.

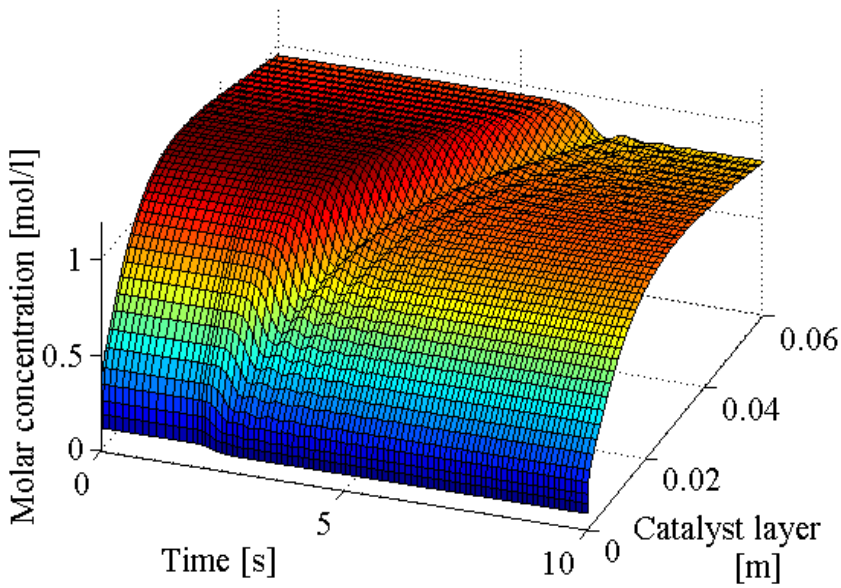

Figure 6-0-6 Dynamic response of hydrogen concentration for a step decrease of $\Delta C_{glycerol}$=-30%

Chapter 7. Hydrogen based power generation from glycerol

7.2. 300 MW_{th} Hydrogen production from glycerol reforming

This subchapter presents four different conceptual designs for hydrogen production from bio-glycerol reforming, and the first three Cases have two subdivision:

Case 1a: Hydrogen production from bioglycerol steam reforming without carbon capture;

Case 1b: Hydrogen production from bioglycerol steam reforming with carbon capture.

Case 2a: Hydrogen production from bioglycerol autothermal reforming with O_2 and without carbon capture;

Case 2b: Hydrogen production from bioglycerol autothermal reforming with O_2 and with carbon capture.

Case 3a: Hydrogen production from bioglycerol autothermal reforming with air and without carbon capture;

Case 3b: Hydrogen production from bioglycerol autothermal reforming with air and with carbon capture.

Case 4: Hydrogen production by direct glycerol chemical looping conversion.

All evaluated plant options were designed to produce 300 MW_{th} hydrogen based on lower heating value (10.8 MJ/Nm^3), this corresponds to 100,000 Nm^3/h, with almost null net power output. The power generated within the plant is mainly used for covering the ancillary consumption; this is also the case for the steam generated in the plant[1].

The fuel used in this analysis is the crude glycerol residues from biodiesel production. The fuel composition is the following (% wt.): 52.49% glycerol, 9.99% methanol, 14.49% methyl oleate and 23.00% water. Ilmenite ($FeTiO_3$) was used as oxygen carrier for chemical looping Case 4 [2]. The case studies presented in this subchapter were modeled and simulated using CHEMCAD software [3].
The main plant characteristics for hydrogen production based on crude glycerol reforming with/without CCS and direct chemical looping and theirs design assumptions used in the modeling are presented in **Error! Not a valid bookmark self-reference.** [4-7].

Table 7-0-1 Main plant design characteristics

Bio-fuel fed and preheating	Fuel composition: 52.5% crude glycerol; 10% biomethanol; 14.5% methyl oleate Bio-fuel preheating: 400-500 °C
Reformer	Ni-based catalyst Pressure: 30 bar Pressure drop: 1 bar Outlet temperature: 850 °C Thermal mode: heat exchanger/ autothermal
Heat exchangers	ΔT_{min}= 10 °C Pressure drop: 1% of inlet pressure
Heat recovery steam generation	Two steam pressure levels: Steam turbine isoentropic efficiency: 85%
Tail gas expander	Tail gas preheating before expansion: 230 °C Outlet pressure: 1.5 bar Expander efficiency: 70%
Pressure Swing Adsorption (PSA)	Purified hydrogen: > 99.95% (vol.) Purification yield: 75.0000 Tail gas pressure: 1.5 bar
CO_2 compression and drying	Delivery pressure: 120 bar 4 compression stages with intercooling Compressor efficiency: 85% Drying solvent: TEG (Tri-ethylene-glycol) Captured CO_2 quality specification (%vol.): >…% CO_2; <…ppm CO; <… H_2O; <100 ppm H_2S; <…% other gases
Carbon capture unit (Cases 1b, 2b and 3b)	Solvent: Methyl-diethanol-amine (MDEA)
Carbon capture unit (Case 4)	Oxygen carrier: ilmenite Fuel reactor parameters: 28 bar/ 700 °C Steam reactor parameters: 26 bar/ 715 °C Air reactor parameters: 24 bar/ 985 °C Thermal mode: adiabatic

The definitions of the key performance indicators, used in the comparison of various cases, are presented in the next section.

Glycerol dry LHV is calculates as follows:

$$LHV_{dry} = \frac{\sum(Q_{m_i} * LHV_i)}{3600} \quad (1)$$

Crude glycerol LHV is calculates as follows:

$$LHV_{glycerol} = LHV_{dry} * (1 - f) - 2442.5 * f \quad (2)$$

Hydrogen efficiency (η_{H_2}) of crude glycerol reforming is calculates as follows:

$$\eta_{H_2} = \frac{hydrogen\ thermal\ energy\ [MW]}{crude\ glycerol\ thermal\ energy\ [MW]} * 100 \quad (3)$$

Net electrical efficiency (η_{net}) of crude glycerol reforming shows overall plant performance in term of electricity conversion process, they are calculated with the formula:

$$\eta_{net} = \frac{net\ power\ output\ [MW]}{crude\ glycerol\ thermal\ energy\ [MW]} * 100 \quad (4)$$

Cumulative efficiency ($\eta_{cumulative}$) of crude glycerol reforming is calculated by adding net electrical efficiency and hydrogen efficiency:

$$\eta_{cumulative} = \eta_{net} + \eta_{H_2} \quad (5)$$

Carbon capture rate (CCR) of crude glycerol reforming is calculated considering the molar flow of captured carbon dioxide divided by carbon molar flow from the feedstock (bio-glycerol):

$$CCR = \frac{captured\ CO_2\ molar\ flow\ [kmole/h]}{crude\ glycerol\ carbon\ molar\ flow\ [kmole/h]} * 100 \quad (6)$$

Specific CO_2 emission (SE_{CO_2}) of crude glycerol reforming is calculated considering the emitted CO_2 mass flow for each MW of hydrogen and power co-generated:

$$SE_{CO_2} = \frac{emitted\ CO_2\ mass\ flow\ [kg/h]}{net\ power\ output\ [MW] + hydrogen\ energy\ [MW]} \quad (7)$$

Table 7-0-2 Overall technical plant performance indicators

Main plant data	Units	Case 1a	Case 1b	Case 2a	Case 2b	Case 3a	Case 3b	Case 4
Bioglycerin flow rate	t/h	110.44	110.44	136.42	136.42	136.42	136.42	108.85
Bioglycerin LHV	MJ/kg	15.26	15.26	15.26	15.26	15.26	15.26	15.26
Feedstock thermal energy-LHV(A)	MW_{th}	468.14	468.14	578.29	578.29	578.29	578.29	461.40
Steam turbine output	MW_e	23.75	17.00	53.11	41.60	53.11	41.60	16.48
Expander power output	MW_e	2.77	1.52	2.83	1.37	2.83	1.37	103.06
Gross electric	MW_e	26.52	18.52	55.94	42.97	55.95	42.97	119.55

power output(B)								
ASU power consumption	MW_e	0	0	11.25	11.26	10.90	10.90	0
Reformer island power consumption	MW_e	0.11	0.11	0.13	0.13	0.13	0.13	78.27
Carbon capture + CO_2 drying and compression	MW_e	0	7.17	0	7.17	0	7.17	3.07
Hydrogen compression	MW_e	3.88	3.99	3.86	3.99	3.86	3.99	3.97
Power island power consumption	MW_e	0.37	0.32	0.56	0.65	0.56	0.65	0.13
Total ancillary power consumption (C)	MW_e	4.36	11.60	15.80	23.20	15.47	22.85	85.45
Hydrogen output (D)	MW_{th}	300	300	300	300	300	300	300
Net electric power output (E=B-C)	MW_e	22.16	6.92	40.14	19.77	40.48	20.11	34.09
Hydrogen efficiency (D/A*100)	%	64.08	64.08	51.87	51.87	51.87	51.87	65.01
Net electrical efficiency (E/A*100)	%	4.73	1.47	6.94	3.41	7.00	3.47	7.38
Cumulative energy efficiency	%	68.81	65.56	58.81	55.28	58.87	55.35	72.40
Carbon capture rate	%	0	70.21	0	69.51	0	56.84	97.55
Specific CO_2 emissions (hydrogen and	Kg/MWh	445.28	139.05	520.93	237.80	520.40	237.54	10.34

power)

The chemical looping concept presents comparable cumulative energy efficiency with steam reforming without carbon capture concept. Case 4 have higher carbon capture rate than Case 3b (with >27%). In the case of specific CO_2 emissions the chemical looping option has the lowest value.
In each evaluated carbon capture case, quality specification of captured CO_2 stream was calculated.

7.3. Pinch analysis for hydrogen production at industrial scale from different conceptual design from

This section presents results of PINCH analysis for hydrogen production at industrial scale for the process of reforming the crude glycerol. These results are obtained by using the MATLAB simulation program.

In Figure 7-0-1 are presented to hot and cold flows temperature ranges of direct chemical looping of crude glycerol. Composite curves for CCS unit of hydrogen production by direct chemical looping of crude glycerol conversion with include CO_2 storage is presented in Figure 7-0-1-b. In Figure 7-0-1-b you can see that it not reached PINCH point. In each heat exchanger of Case 4 does not touch the PINCH point and a minimum temperature of 5ºC between the temperature of the exhaust flow hot and cold streams.

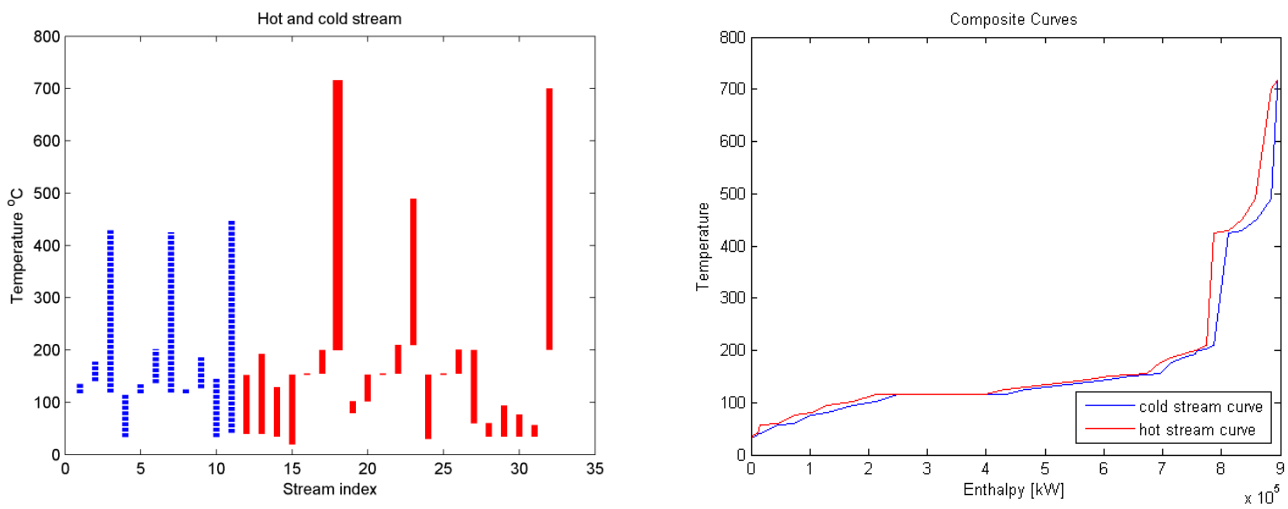

a) b)

Figure 7-0-1 Glycerol chemical looping to hydrogen production (equivalent 300MW$_{th}$)

7.4. Hydrogen based power generation from different conceptual design from glycerol

The following hydrogen-based power generations from crude glycerol reforming concepts were investigated in this subchapter:

Case 1a: Hydrogen-based power generation from bioglycerol steam reforming without carbon capture;

Case 1b: Hydrogen-based power generation from bioglycerol steam reforming with carbon capture.

Case 2a: Hydrogen-based power generation from bioglycerol autothermal reforming with O_2 and without carbon capture;

Case 2b: Hydrogen-based power generation from bioglycerol autothermal reforming with O_2 and with carbon capture.

Case 3a: Hydrogen-based power generation from bioglycerol autothermal reforming with air and without carbon capture;
Case 3b: Hydrogen-based power generation from bioglycerol autothermal reforming with air and with carbon capture.
Case 4: Hydrogen-based power generation by direct glycerol chemical looping conversion.

The main design characteristics of various plant sub-systems are presented in Table 7-0-3[4-7]. The case studies presented in this paper were modeled and simulated using CHEMCAD software [8].

Table 7-0-3 Main plant design characteristics

Bio-fuel fed and preheating	Fuel composition: 52.5% bio-glycerol; 10% bio-methanol; 14.5% methyl oleate Bio-fuel preheating: 400-500 °C
Reformer	Ni-based catalyst Pressure: 30 bar Pressure drop: 1 bar Outlet temperature: 850 °C Thermal mode: heat exchanger/ autothermal
Heat exchangers	ΔT_{min}= 10 °C Pressure drop: 1% of inlet pressure
Heat recovery steam generation	Two steam pressure levels: Steam turbine isoentropic efficiency: 85%
Tail gas expander	Tail gas preheating before expansion: 230 °C Outlet pressure: 1.5 bar Expander efficiency: 70 %
Pressure Swing Adsorption (PSA)	Purified hydrogen: > 99.95 % (vol.) Purification yield: 65 – 85 % Tail gas pressure: 1.5 bar
Carbon capture unit (Cases 1b, 2b, 3b)	Solvent: Methyl-diethanol-amine (MDEA) Solvent regeneration: thermal Absorption: desorption cycle
Carbon capture unit (Case 4)	Oxygen carrier: ilmenite Fuel reactor parameters: 28 bar/ 700 °C Steam reactor parameters: 26 bar/ 715 °C Air reactor parameters: 24 bar/ 985 °C Thermal mode: adiabatic

The definitions of the key performance indicators, used in the comparison of various cases, are presented in the next section.

Crude glycerol dry LHV is calculates as follows:

$$LHV_{dry} = \frac{\sum Q_{m_i} * LHV_i}{3600} \quad (8)$$

Crude glycerol LHV is calculates as follows:

$$LHV_{glycerol} = LHV_{dry} * (1 - f) - 2442.5 * f \quad (9)$$

Hydrogen efficiency (η_{H_2}) of hydrogen-based power generation from crude glycerol is calculates as follows:

$$\eta_{H_2} = \frac{hydrogen\ thermal\ energy\ [MW]}{crude\ glycerol\ thermal\ energy\ [MW]} * 100 \quad (10)$$

Net electrical efficiency (η_{net}) of hydrogen-based power generation from crude glycerol shows overall plant performance in term of electricity conversion process, they are calculated with the formula:

$$\eta_{net} = \frac{net\ power\ output\ [MW]}{crude\ glycerol\ thermal\ energy\ [MW]} * 100 \quad (11)$$

Carbon capture rate (CCR) of hydrogen-based power generation from crude glycerol is calculated considering the molar flow of captured carbon dioxide divided by carbon molar flow from the feedstock (crude glycerol):

$$CCR = \frac{captured\ CO_2\ molar\ flow\ [kmole/h]}{crude\ glycerol\ carbon\ molar\ flow\ [kmole/h]} * 100 \quad (12)$$

Specific CO_2 emission (SE_{CO_2}) of hydrogen-based power generation from crude glycerol is calculated considering the emitted CO_2 mass flow for each MW of hydrogen and power co-generated:

$$SE_{CO_2} = \frac{emitted\ CO_2\ mass\ flow\ [kg/h]}{net\ power\ output\ [MW] + gas\ turbine\ [MW]} \quad (13)$$

Table 7-0-4 Overall technical plant performance indicators

Main plant data	Units	Case 1a	Case 1b	Case 2a	Case 2b	Case 3a	Case 3b	Case 4
Crude glycerol flowrate	t/h	273.95	273.95	319.90	319.90	319.90	319.90	296.72
Crude glycerol LHV	MJ/kg	15.26	15.26	15.26	15.26	15.26	15.26	15.26
Feedstock thermal energy-LHV(A)	MW_{th}	1161.25	1161.25	1356.02	1356.02	1356.02	1356.02	1257.79
Steam turbine output	MW_e	186.68	182.22	221.18	211.53	218.99	209.26	204.78
Expander power output	MW_e	6.76	3.25	5.54	2.74	9.99	7.11	314.78
Gas turbine	MW_e	334	334	334	334	334	334	334
Gross electric power output(B)	MW_e	527.44	519.48	560.72	548.27	562.98	550.38	853.56
ASU power consumption	MW_e	0	0	26.41	26.41	0	0	0
Reformer island power consumption	MW_e	0.27	0.27	0.32	0.32	36.12	36.12	236.66
Carbon capture + CO_2 drying and	MW_e	0	18.76	0	24.68	0	25.43	8.38

compression								
Power island power consumption	MW_e	2.99	2.99	3.28	3.27	3.25	3.24	2.66
Hydrogen compression	MW_e	0	0	0	0	0	0	10.84
N_2 compression	MW_e	19.46	19.46	19.46	19.46	19.46	19.46	19.46
Total ancillary power consumption (C)	MW_e	22.73	41.49	49.48	74.15	58.84	84.27	278.02
Net electric power output (E=B-C)	MW_e	504.70	477.98	511.24	474.11	504.13	466.10	575.54
Net electrical efficiency (E/A*100)	%	43.46	41.16	37.70	34.96	37.17	34.37	45.75
Carbon capture rate	%	0	75.41	0	85.09	0	87.83	97.55
Specific CO_2 emissions (hydrogen and power)	Kg/MWh	707.48	157.76	815.18	88.83	826.67	65.96	18.50

The chemical looping concept presents comparable cumulative energy efficiency with steam reforming without carbon capture concept. Case 4 have higher carbon capture rate than Case 3b (with >2.3%). In the case of specific CO_2 emissions the chemical looping option has the lowest value.
In each evaluated carbon capture case, quality specification of captured CO_2 stream was calculated .

7.5. Pinch analysis for hydrogen-based power generation from different conceptual design from crude glycerol

This section presents results of PINCH analysis for hydrogen-based power generation at industrial scale for the process of reforming the bioglycerol. These results are obtained by using the MATLAB simulation program.

In Figure 7-0-2-a are presented to hot and cold flows temperature ranges of hydrogen-based power generation with direct chemical looping of crude glycerol. Composite curves for CCS unit of hydrogen-based power generation by direct chemical looping of crude glycerol conversion with include CO_2 storage is presented in Figure 7-0-2-b. In Figure 7-0-2-b you can see that it reaches PINCH point around the temperature of 50°C. In each heat exchanger of Case 4 does not touch the PINCH point and a minimum temperature of 5°C between the temperature of the exhaust flow hot and cold streams.

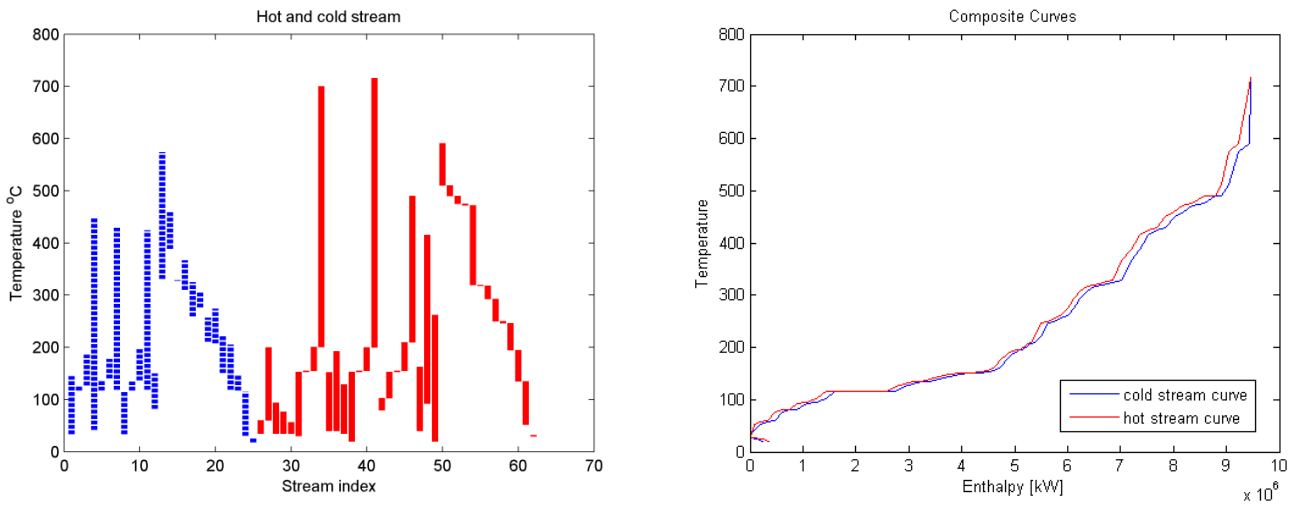

a) b)

Figure 7-0-2 Hydrogen based power generation from chemical looping of glycerol

Reference (summary):

1. Zs. Tasnadi-Asztalos, P.-S. Agachi, C.-C. Cormos; *Int J Hydro Energy*, **2015,** 40, 22, 7017.
2. Zs. Tasnadi-Asztalos, A. Imre-Lucaci, C.C. Cormos, A.M. Cormos, M.D. Lazar, P.S. Agachi, *Comput Aided Chem Eng*, **2014**, 33, 1735.
3. C.C. Cormos, *Int J Hydrog Energy*, **2014**, 39, 5597.
4. H. Chen, Y. Ding, N. Cong, B. Dou, V. Dupont, M. Ghadiri, et al., *Renew Energy* **2011**, 36, 779.
5. Wang C, Dou B, Chen H, Song Y, Xu Y, Du X, et al.,*Int J Hydrog Energy* **2013**, 38, 3562.
6. B. Dou, Y. Song, C. Wang, H. Chen, M. Yang, Y. Xu, *Appl Energy*, **2014**,130, 342.
7. S. Shao, A.W. Shi, C.L. Liu, R. Yang, W.S. Dong, *Fuel Process Technol*, **2014**,125,1.
8. M. Bade, S.Bandyopadhyay, *Appl Therm Eng*, **2015**;78,118.

Part IV – Conclusions

Chapter 8. General conclusions

8.1 Conclusions and future work perspective

Maximum concentration of hydrogen which can be obtained from the steam reforming of crude ethanol according to thermodynamic study is 75% mole at 600°C, 1bar pressure respectively at water:ethanol molar ratio 25:1.

The most favorable conditions for steam reforming of bioethanol is in the temperature range 700-800°C, low pressure and at a water:ethanol molar ratio 25:1.

The second part of this chapter describes the research work done on the thermodynamic analysis of the process of bioethanol steam reforming. Also, for a kinetic model reported in the literature, the kinetic constants were recalculated to adjust the model to the experimental data obtained by using 10%Ni-Al_2O_3 catalyst in isothermal conditions at 350°C. The thermodynamic analysis takes into account the main chemical species involved in the reactions (reactants as well as products). Following

the thermodynamic study has resulted that the maximum concentration of H_2 was obtained at the molar ratio of water:ethanol 3:1, temperature of 550°C and 1 bar pressure.

The adjustment of the LHHW kinetic model based on the experimental data obtained in a laboratory plant succeeds to determine the kinetic constants of the process but the fitness of the model was rather poor. In order to improve the kinetic model accuracy, new experiments need to be considered and more parameters of the model have to be included in the adjustment process.

The best conceptual design for hydrogen from crude ethanol is the chemical looping conversion with cumulative electrical efficiency 67%, carbon capture rate 93.54% and with 1.79 Kg/ MWh CO_2 emissions.

The best conceptual design for power generation based on hydrogen from bioethanol is the chemical looping conversion with net electrical efficiency 43.5%, carbon capture rate 93.8% and with 35.8 Kg/ MWh CO_2 emissions.

A thermodynamic analysis and literature validation of bioglycerol catalytic steam reforming using Ni/Al_2O_3 catalyst for hydrogen production is presented in this article. The chapter presents the results of a detailed thermodynamic analysis, for a complete overview of the chemical process. Following thermodynamic study the most important factors which influence the steam reforming of bioglycerol are the water:bioglycerol molar ratio and the temperature.

The concentrations of the main product (H_2) at lower temperature are smaller than the ones at higher temperature due to by-products formation (methane). The concentration of H_2 obtained in the process using water:bioglycerol molar ratio of 10 (higher than the stoichiometric ratio) is higher than the one at water:bioglycerol molar ratio of 3:1.

The simulation results were used to assess the overall process parameters such as chemical species concentration profiles along the glycerol steam reforming reactor. The dynamic mathematical model of hydrogen production from bioglycerol steam reforming in a continuous flow tubular reactor presents similar results with the literature date. The main component (hydrogen) concentration is increasing with the flow rate decreasing. If the initial concentration of the reactant increases the hydrogen concentration is also increase.

The best conceptual design for hydrogen from crude glycerol is the chemical looping conversion with cumulative electrical efficiency 72%, carbon capture rate 97.55% and with 10.34 Kg/ MWh CO_2 emissions.

The best conceptual design for power generation based on hydrogen from bioglycerol is the chemical looping conversion with net electrical efficiency 46%, carbon capture rate 97.5% and with 18.5 Kg/ MWh CO_2 emissions.

8.2 Personal contributions

I conducted a thermodynamic study of the catalytic steam reforming of bioethanol at a largest domain of temperature, pressure and water:ethanol molar ratio than I found in literature. After thermodynamic study of steam reformation of bioethanol have conducted an analysis of the kinetics of the process. To realize the thermodynamic study of catalytic steam reforming of ethanol and the kinetic analyze of the catalytic steam reforming of ethanol I was helped by Árpád Imre-Lucaci. Results from the simulation were presented in the following works:

- **Zsolt Tasnadi-Asztalos,** Arpad Imre-Lucaci, Ana-Maria Cormos, Mihaela Diana Lazar, Paul-Serban Agaci; Themodynamic study and kinetic modeling of bioethanol steam reforming; *Studia Universitatis Babes - Bolyai, Chemia,*LVIII, 4, 101-112, Cluj-Napoca, Romania, 2013
- **Zsolt Tasnadi-Asztalos,** Ana-Maria Cormos, Árpád Imre-Lucaci, and Calin-Cristian Cormos; Thermodynamic evaluation of hydrogen production via bioethanol steam reforming; AIP Conference Proceedings 1565, 175 (2013).

I conducted a thermodynamic study of the catalytic steam reforming of bioglycerol at a largest domain of temperature, pressure and water:ethanol molar ratio than I found in literature. Results from the simulation were presented in the next work:

- **Zsolt Tasnadi-Asztalos**, Arpad Imre-Lucaci, Calin-Cristian Cormos, Ana-Maria Cormos, Mihaela-Diana Lazar, Paul-Serban Agachi; Thermodynamic Study of Hydrogen Production via Bioglycerol Steam Reforming; Proceedings of the 24th European Symposium on Computer Aided Process Engineering – ESCAPE 24 June 15-18, 2014, Budapest, Hungary

I realize the dynamic simulation of hydrogen production from bioglycerol steam reforming in a continuous flow tubular reactor. To realize this study was helped by Ana-Maria Cormos. The results from this simulation were presented in the next work:

- **Zsolt Tasnadi-Asztalos,** Calin-Cristian Cormos, Ana-Maria Cormos, Diana Lazar, Paul-Serban Agachi; Dynamic simulation of hydrogen production from bioglycerol steam reforming in a continuous flow tubular reactor; 10th Conference on Sustainable Development of Energy, Water and Environment Systems, September 27 - October 2, 2015, Dubrovnik, Croatia

With Calin-Cristian Cormos, we developed different conceptual design for hydrogen production from glycerol reforming. The results from this conceptual design for hydrogen production from glycerol were presented in the next work:

- **Zsolt Tasnadi-Asztalos**, Paul-Serban Agachi, Calin-Cristian Cormos; Evaluation of energy efficient low carbon hydrogen production concepts based on glycerol residues from biodiesel production; International Journal of Hydrogen Energy, Volume 40, Issue 22, 15 June 2015, Pages 7017-7027.

With Calin-Cristian Cormos, we developed different conceptual design for hydrogen-based power generation from bioethanol reforming. The results from this conceptual design for hydrogen-based power generation from bioethanol were presented in the next work:

- **Zsolt Tasnadi-Asztalos**, Calin-Cristian Cormos, and Paul-Serban Agachi; Hydrogen-based power generation from bioethanol steam reforming; AIP Conference Proceedings 1700, 050001 (2015).

I wrote a simulation program in Matlab to make it easier the PINCH analyze using the data from the CHEMCAD process simulator program.

Using the different conceptual design for hydrogen-based power generation from bioethanol reforming, I realize different conceptual design hydrogen-based power generation from bioglycerol reforming which was presented in this thesis.

8.3 List of publications

I. Calin-Cristian Cormos, Arpad Imre-Lucaci, Ana-Maria Cormos, **Zsolt Tasnadi-Asztalos**, Mihaela Diana Lazar; Conceptual design of hydrogen production process from

bioethanol reforming; *Proceedings of the 23rd European Symposium on Computer Aided Process Engineering (ESCAPE 23 June 9-12, 2013, Lappeenranta, Finland)*

II. **Zsolt Tasnadi-Asztalos,** Arpad Imre-Lucaci, Ana-Maria Cormos, Mihaela Diana Lazar, Paul-Serban Agaci; Themodynamic study and kinetic modeling of bioethanol steam reforming; *Studia Universitatis Babes - Bolyai, Chemia*,LVIII, 4, 101-112, Cluj-Napoca, Romania, 2013.

III. **Zsolt Tasnadi-Asztalos,** Ana-Maria Cormos, Árpád Imre-Lucaci, and Calin-Cristian Cormos; Thermodynamic evaluation of hydrogen production via bioethanol steam reforming; AIP Conference Proceedings 1565, 175 (2013).

IV. **Zsolt Tasnadi-Asztalos**, Arpad Imre-Lucaci, Calin-Cristian Cormos, Ana-Maria Cormos, Mihaela-Diana Lazar, Paul-Serban Agachi; Thermodynamic Study of Hydrogen Production via Bioglycerol Steam Reforming; Proceedings of the 24th European Symposium on Computer Aided Process Engineering – ESCAPE 24 June 15-18, 2014, Budapest, Hungary

V. **Zsolt Tasnadi-Asztalos**, Paul-Serban Agachi, Calin-Cristian Cormos; Evaluation of energy efficient low carbon hydrogen production concepts based on glycerol residues from biodiesel production; International Journal of Hydrogen Energy, Volume 40, Issue 22, 15 June 2015, Pages 7017-7027

VI. Monica Dan, Maria Mihet, **Zsolt Tasnadi-Asztalos**, Arpad Imre-Lucaci, Gabriel Katona, Mihaela Diana Lazar; Hydrogen production by ethanol steam reforming on nickel catalysts: Effect of support modification by CeO2 and La2O3; Fuel 147 (2015) 260–268;

VII. **Zsolt Tasnadi-Asztalos,** Calin-Cristian Cormos, Ana-Maria Cormos, Diana Lazar, Paul-Serban Agachi; Dynamic simulation of hydrogen production from bioglycerol steam reforming in a continuous flow tubular reactor; 10th Conference on Sustainable Development of Energy, Water and Environment Systems, September 27 - October 2, 2015, Dubrovnik, Croatia

VIII. **Zsolt Tasnadi-Asztalos**, Calin-Cristian Cormos, and Paul-Serban Agachi; Hydrogen-based power generation from bioethanol steam reforming; AIP Conference Proceedings 1700, 050001 (2015);